CHARACTERIZATION OF PIGMENTS FROM *Spinacea oleracea*, *Beta vulgaris*, AND *Rubus fruticosus* FOR APPLICATION IN DYE-SENSITIZED SOLAR CELLS

MORONGE ZACHARIAH KIBAGENDI

A Thesis Submitted to the Graduate School in Partial Fulfilment of the Requirements for the Master of Science Degree in Physics of Egerton University

EGERTON UNIVERSITY

NOVEMBER, 2025

DECLARATION AND RECOMMENDATION

Declaration

This thesis is my original work and has not been presented in this University or any other for the award of a degree.

Signature: …  …….Date: November 2, 2025…

Moronge Zachariah Kibagendi

SM13/13675/19

Recommendation

This thesis has been submitted with our approval as university supervisors.

Signature:…  ……. Date: November 3, 2025…

Dr Duke Oeba, PhD
Department of Physics
Egerton University

Signature:…  ……Date: November 3, 2025…

Dr Charles Muga, PhD
Department of Physics,
Egerton University

COPYRIGHT

DEDICATION

With gratitude, I thank my parents, Samson Moronge and the late Mary Moraa, for their continuous guidance that inspired my progress throughout my academic journey.

ACKNOWLEDGEMENTS

With deep gratitude, I thank God for His constant love and protection during my master's studies. I am thankful to Egerton University for giving me the opportunity to pursue my master's programme. I appreciate the United Nations Educational, Science and Cultural Organization (TWAS-UNESCO) supporting my project under Grant Agreement NO. 4500474973. I am grateful to have had the unwavering support of my supervisors, Dr. D. Oeba and Dr. C. Muga, of Egerton University throughout the research. They were instrumental in helping me succeed in identifying topics, offering constructive criticism, and writing my thesis. I also wish to thank my wife, Mercy Mumo, and my dear son, Logan Lowen, who have been with me throughout this learning process, so supportive, loving, and patient. My deepest appreciation also goes to Seth Osumba from the Chemistry Department and Fred Mukwa from the Physics Department of Egerton University, without whom it would have been hard to characterize the dye extracts.

ABSTRACT

In response to growing energy consumption motivated by demographic growth, renewable energy technologies must rapidly advance and reinvent. Among sustainable energy innovations, solar energy is notably a universally accessible resource. Dye-sensitized Solar Cells (DSSCs) exploit solar energy and are preferred due to lower fabrication cost and eco-friendliness. Reduced optical absorption is a major drawback in utilizing DSSCS. To mitigate these challenges, co-sensitization (utilization of multiple dyes sensitizers in fabricating DSSCs) is employed to broaden the absorption spectrum. In this research, dyes from *Spinacea oleracea* leaves, *Rubus fruticosus* fruits, and *Beta vulgaris* roots are co-sensitized. The impact of annealing temperature and dye-loading time of TiO_2 films on the photovoltaic parameters of DSSC were evaluated. Dye's optical absorption spectra were characterized using an ultraviolet-visible spectrophotometer (400-800 nm). Absorption spectra for *Spinacea oleracea* extract were detected at 400-480 nm (blue region) and 640-700 nm (red region), respectively, and hence reflecting green (chlorophyll). The maximum absorption *for Beta vulgaris* dye was within the 500-560 nm region, attributed to betanin pigments. Dyes extracted from *Rubus fruticosus* fruits revealed a wide absorption in the region of 450-650 nm that was linked to the presence of anthocyanin. The mixture dye showed a broad optical absorption band as compared to individual dyes. Fourier Transform Infrared (FTIR) spectroscopy was applied in confirming the presence of functional groups in dye extracts. DSSCs photovoltaic characteristics were assessed from a solar simulator under a standard AM 1.5 G illumination. According to the experiment results, the optimal annealing temperature and dye-loading time on TiO_2 film were 450 °C and 40 h, respectively, obtained from the performance of fabricated DSSCs. Open-circuit voltage, short-circuit current density, fill factor, and power conversion efficiency of 0.59 V, 3.6 mA/cm^2, 74.78 %, and 1.58 %, respectively, were obtained. These results were also a result of co-sensitizing all three dyes (chlorophyll, anthocyanin, and betanin) in a 1:1:1 volume ratio. The research concludes that natural dyes are feasible, inexpensive, and ecofriendly sensitizers for DSSC, though their PCE remain restricted by poor photon absorption properties. Mixing chlorophyll, betanin, and anthocyanin improves solar spectra coverage, exhibiting the promise of blending natural dyes to augment DSSC performance. Purification of dye extracts, co-sensitization of natural dyes with ruthenium dyes, and annealing TiO_2 film after dye loading can be explored in future to improve the quality of dye extracts and TiO_2 film for efficient DSSC development.

TABLE OF CONTENTS

LIST OF TABLES

LIST OF FIGURES

LIST OF ABBREVIATIONS AND ACRONYMS

a.u	Arbitrary units
CE	Counter Electrode
Cya-3-glu	Cyanidine-3-o-glucoside
DSSCs	Dye-sensitized Solar Cells
FF	Fill Factor
FTO	Fluorine Doped Tin Oxide
I_{SC}	Short circuit current
ITO	Indium Tin Oxide
J-V	Current density-Voltage
J_{SC}	Short circuit current density
OPV	Organic Photovoltaic
PA	Photo Anode
PCE	Power Conversion Efficiency
PSCs	Perovskite Solar Cells
Pt	Platinum
PV	Photovoltaic
Rpm	Revolution per minute
SA	Surface Area

LIST OF SYMBOLS

A_λ	Absorbance at a particular wavelength
ε	Molar absorption coefficient
B	Anthocyanin
C	Betanin
A	Chlorophyll
h	Planck's constant
ν	Frequency
λ	Wavelength
l	Cuvette thickness
c	Pigment concentration

CHAPTER ONE
INTRODUCTION

1.1 Background information

With the growing energy demand, there has been a recent surge in researchers dedicated to discovering clean and sustainable energy (Kusumawati *et al.*, 2025). The Seventh Goal of the United Nations' Sustainable Development Goals (SDGs) intends to ensure universal access to affordable, dependable, regenerative, and contemporary energy by 2030. In 2023, sustainable energy sources contributed 30.3 % to global electricity production, up from 29.4 % in 2022. This share is projected to increase by 60 % by 2070. The other 69.7 % corresponded to fossil fuels, nuclear energy, and other non-renewables (Al-Rikabi *et al.*, 2025). The rapid depletion of fossil fuel reserves and the harsh environmental pressures posed by burning these fuels have accelerated the modernization of energy generation and the adoption of energy from green sources (Wang & Azam, 2024). No alternative energy source is plentiful as solar energy. Nevertheless, the efficient conversion of light into electricity remains a persistent challenge that has been managed by embracing photovoltaic (PV) cells (Andualem & Demiss, 2018).

Crystalline silicon solar cells (converts solar radiation into electricity) to date lead the market sale of PVs by 85 %, boasting a power conversion efficiencies (PCEs) of up to 27.30 % (Liang *et al.*, 2025). However, despite high PCE, the substantial manufacturing cost of silicon solar photovoltaic poses significant affordability challenges for a substantial portion of the global population (Machín & Márquez, 2024). These challenges have driven the advancement of alternative PV technologies that offer desirable properties such as lightweight design, flexibility, and low module cost (Meng *et al.*, 2018). Among these alternatives, dye-sensitized solar cells (DSSCs) are particularly intriguing compared to silicon solar cells as they are less costly, light in weight, portable, easy to fabricate, and flexible (Kumar & Naidu, 2021).

The composition of a DSSC primarily includes a transparent conductive substrate (Tamilselvan & Shanmugan, 2024), semiconductor nanostructure, dye photosensitizer, a redox liquid electrolyte, and catalyst-coated counter electrode (Magiswaran *et al.*, 2021). The dye is adsorbed onto the surface of TiO_2 semiconductor, forming a photoanode that enhances optical energy absorption (Pallikkara & Ramakrishnan, 2021). Since the research by O'regan and Grätzel (1991), pioneering design of high-performance DSSCs sensitized with ruthenium dyes in 1991 , these cells have since enticed many researchers' interests, warranting further study (Rahman *et al.*, 2023). DSSCs' efficiency is notably affected by dye selection, accounting for approximately 50% of the fabrication costs (Aslam *et al.*, 2020). Metal complexes and organic and natural (organic) dyes are the most commonly used sensitizers (Jabeen *et al.*, 2025).

Hitherto, ruthenium-based metal complex dyes have performed a momentous task in the functioning of DSSCs owing to a superior absorption rate of solar energy and appropriate functional groups that facilitate bonding with metal oxide semiconductors (Rahman *et al*., 2023). Notably, DSSCs sensitized with metal complex dyes have achieved a remarkable efficiency exceeding 11% (Rajaramanan *et al.*, 2023). Nevertheless, these dyes are pricy and unstable at high temperatures, so searching for alternative sensitizers is both necessary and inevitable (Wang *et al.*, 2025).

Natural plant-based dyes are regarded as a substitute for ruthenium-based dyes as they are simple to extract and synthesize (Ponnambalam *et al.*, 2023). Anthocyanin, betalain (Vallejo *et al.*, 2025), carotenoid, and chlorophyll (Semalti & Sharma, 2020) extracted from various plant parts have been employed as photosensitizers in DSSCs (Hezarkhani & Ghadari, 2025). The utilization of these dyes is aimed at achieving renewability, and dependability and supporting an environment that is friendly (Dhorkule *et al.*, 2024).

Lately, significant attempts have been put forth to synthesize efficient dye sensitizers which contribute to DSSCs fabrication (Tamilselvan & Shanmugan, 2024). The optical absorption spectrum of natural DSSCs is narrow, which leads to minimum photon absorbance, and hence poor sensitization of dyes which leads to lower efficiency (Baby *et al.*, 2022). To boost the efficiency of DSSCs, the photon absorption properties of natural dyes ought to be adjusted to exhibit optimal performance throughout the visible and near-infrared spectrum (Malhotra *et al.*, 2024). Co-sensitization of dyes presently a highly buzzling subject in the fabrication of DSSCs (Singh *et al.*, 2022), attracting significant attention from researchers (Krishna *et al.*, 2017). In this case, semiconductor thin films are usually co-adsorbed with two or more different dyes with different optical behavior (Khajavian *et al.*, 2020).

Many studies have explored co-sensitized DSSCs as a strategy to broaden the absorption spectra and enhance overall performance (Krishna *et al*., 2017). Co-sensitization is now a well-established approach that ought to be adopted in achieving panchromatic shift and to further elevate DSSC performance. Panchromatic shift is the widening of the absorption wavelength by dye sensitizers so as to absorb sunlight across a wide scope of solar spectrum. For instance, Ezike *et al.*, (2021b) documented a wide absorption spectrum and a PCE of 1.14 % in DSSC made by combining anthocyanin and chlorophyll dyes. Similarly, Patni *et al*. (2020) realized a PCE of 3.73 % using a combination of three natural photosensitizers obtained from *H. sabdarifa, B. vulgaris* and *S. oleracea*. According to Sreeja and Pesala (2018), a PCE of 0.601 % was obtained by mixing natural dyes obtained from red beetroot and spinach in an optimized ratio. In another study, an efficiency of 0.20 % was obtained by combining *Opuntia dillenii*

and *Tamarindus indica* dyes, which is higher than the 0.14 % achieved with individual *Tamarindus indica* (Ramamurthy *et al*., 2016). These results highlight how co-sensitization has been proven to boost the PCE of DSSCs by conquering the impediments induced by the small spectral window of mono sensitizers (Barichello *et al.*, 2024). This amplification can be ascribed to the synergistic effect of improved photon-to-current efficiency (IPCE) and short-circuit current density (Akhtaruzzaman *et al*., 2021). Annealing temperature coupled with dye sensitization time are some of the major variables that control the DSSCs photovoltaic performance (Kandregula *et al.*, 2025).

It is well known that annealing TiO_2 photoanode removes organic binders and solvents, improves particle connectivity, reinforces adhesion to the FTO, and improves crystallinity of TiO_2 nanoparticles (Lukong *et al.*, 2022). Presently, nanoporous TiO_2 films for DSSCs are synthesized primarily from nanoparticles and annealed at 450 °C (Lin & Chen, 2025). However, from an industrial perspective, reducing the annealing temperature is of great interest, as it can lower fabrication costs and enable the use of flexible plastic substrates (Sreeja & Pesala, 2018). Despite this advantage, TiO_2 films annealed at lower temperatures have demonstrated lower PCE compared to those annealed at higher temperatures (Syrek *et al.*, 2020). In this work, the prospect of dyes based on the chlorophyll, anthocyanin, and betanin extracted from *Spinacia oleracea* (spinach) leaves, *Rubus fruticosus* (blackberry) fruits, and *Beta vulgaris* (beetroot) roots, respectively, were assessed for use in DSSC as sensitizers, both singly and combined. TiO_2-based thin films were fabricated by the doctor blading technique at room temperature on an FTO glass substrate and then annealed at different temperatures to optimize the material's optical properties for application in DSSCs.

Additionally, the impact of dye-adsorbent time on the TiO_2 film layer was examined. The overarching goal is not only to enhance the PCE of assembled DSSCs but also to establish a foundation for future exploration of novel natural sensitizers for the design of low-cost, efficient, and commercially feasible DSSCs. Film's dye adsorption time ought to be optimal to allow for the development of a uniform monolayer of dye leading injection of electrons to the conduction band of TiO_2 semiconductor giving rise to a high J_{SC} and good V_{OC} (Hossain *et al.*, 2018). Due to different dye-sensitized materials exhibiting varying dye-loading rates, the duration of dye adsorption governs the amount and how adsorbing dye particles adhere to the surface; ultimately influencing cell performance (Abdellah, 2025). Moreover, achieving an optimal dye layer is essential. It not only ensures complete coverage of the oxide surface with a monolayer of dye molecules but also minimizes dye aggregation (Wu *et al*., 2025). This

optimal configuration helps suppress the recombination and trapping of charge carriers and facilitates efficient electron injection into the oxide material.

The choice of this natural material for extracting natural dyes was informed by the characteristics of each individual pigment that they contain. Chlorophyll from *Spinacia oleracea* is a porphyrin-based with magnesium ion at the center of the structure. It absorbs light mainly at 400-500 nm and 600-700 nm. This dye has a high absorbance of photons in the visible region of solar spectrum leading to a faster electron injection and is known to generate electric power when used in DSSC fabrication. Anthocyanin from *Rubus fruticosus* are flavonoid pigments that capture light around wavelengths 450- 550 nm in the visible region of solar spectrum. These pigments are PH dependent, nontoxic, widely available and can absorb photons for dye sensitization. Betanin from *Beta vulgaris* on the other hand are found in beetroots from betanin family. Absorb light at 525 nm and can easily harvest solar energy for dye sensitization.

1.2 Statement of the problem

The scarcity of fossil fuels and their adverse environmental impacts during extraction and usage underscores the necessity for an alternative energy source. Solar energy, known for its abundance and environmental sustainability, emerges as a viable solution. Among solar technologies, natural dye-sensitized Solar Cells (DSSCs), stand out as a result of their uncomplicated dye extraction process and readily available, cost-effective raw materials. However, a notable limitation is their narrow optical absorption window, resulting from the use of single natural dyes as sensitizers, poor annealing and inadequate dye loading time for TiO_2 films. The concept of co-sensitization (combining multiple natural dyes as sensitizers), varying annealing temperatures and dye loading time for TiO_2 photoanodes remains largely unexplored. If dyes are optimally co-sensitized, TiO_2 film well annealed, and dye loading time too optimized, this multi-pronged approach could expand the absorption spectrum, improve DSSC efficiency, lower manufacturing expenses, and enhance affordability.

1.3 Objectives

1.3.1 General objective

To extract and optimize pigments from *Spinacea oleracea* leaves, *Beta vulgaris* roots, and *Rubus fruticosus* fruits for co-sensitization in dye-sensitized solar cells and investigate the effect of varying TiO_2 film parameters on the photovoltaic performance of DSSC.

1.3.2 Specific objectives

i. To extract chlorophyll, anthocyanin, and betanin dyes and characterize their functional groups
ii. To determine the optical absorbance of single and blended dye extracts
iii. To evaluate the effects of TiO_2 film dye-loading time on the photovoltaic performance of DSSC
iv. To evaluate the effects of TiO_2 films' annealing temperature on the photovoltaic performance of DSSC

1.4 Research questions

i. What are the effective methods of extracting natural dyes and what are the characteristic functional groups present in these dyes?
ii. What are the optical absorbance characteristics of single and blended dye extracts?
iii. Is there any relationship between the photovoltaic performance of DSSC and TiO2 films' dye-loading time?
iv. What are the effects of the annealing temperature of TiO_2 films on the photovoltaic performance of DSSC?

1.5 Justification

Each day witnesses a surge in worldwide energy consumption, propelled by the expanding population and the escalating energy demand. Diminishing reserves of fossil fuels, primarily utilized for energy generation, have raised concerns and intensified the search for substitute energy sources. Among these, solar energy is distinguished as a clean, renewable, and abundant solution. Harnessing solar power presents an opportunity to mitigate reliance on fossil fuels and curb ecological challenges. Solid-state junction solar photovoltaics at present predominate the field of solar cells due to their superior efficiency. Natural Dye Sensitized Solar Cells (DSSCs) offer cheap and an environmentally friendly option that can help address global warming concerns. However, if natural dyes are applied singly as sensitizers, annealing temperature and dye-loading time for TiO_2 film not optimized, DSSC would develop poor optical absorbance ranges coupled with electron recombination ultimately reducing DSSC power conversion efficiency. This research seeks to extract natural dyes and optimize their mixtures for application in DSSCs as co-sensitizers. Additionally, the study investigates the impact of annealing temperature and dye-loading duration on the TiO_2 films to optimize the performance of DSSC. The results of this study will contribute towards developing cheap and peak-performance DSSCs to drive massive economic advancement. By fabricating

inexpensive, renewable energy harnessing devices, this study contributes head-on to the SDG goal number 7, that purposes to guarantee access to budget-friendly, dependable and clean energy for all. Thus, this research conforms to the global attempts to facilitate sustainable energy remedy, minimize reliance on fossil fuels, and promote environmental conservation.

CHAPTER TWO
LITERATURE REVIEW

2.1 The evolution of solar cells

The photovoltaic effect was pioneered experimentally by French physicist Edmond Becquerel in 1839 (Sharma & Mishra, 2025). At just 19 years old, he fabricated the world's groundbreaking photovoltaic cell (Bulavko, 2024). As part of this investigation, silver chloride was immersed in an acidic solution and powered on while connected to a platinum electrode, producing current and voltage (Ahliouati *et al.*, 2025). For this reason, the photovoltaic effect is referred to as the "Becquerel effect" (Wu *et al*., 2017). The term "Photovoltaic" is a Greek word referring to light and voltaic. Becquerel in 1839 studied photoelectric experiments with liquid state devices (Sharma & Mishra, 2025), where he observed that an electric current was produced when using two platinum electrodes coated with AgCl or AgBr placed in an electrolyte and exposed to light (Sharma & Mishra, 2025).

In 1876, William Adams and Richard Day reported that selenium could be used to produce photoconductivity (Basu, 2024). Following this, the inaugural solar cell was designed in 1883 by Charles Fritts (Sen *et al.*, 2018), who covered selenium with thin layers of gold to form junctions (Hadar *et al.*, 2019). He indicated that the selenium produced a current, "that is continuous, constant, and of notable force with exposure to sunlight" (Sen *et al*., 2018). It is estimated that the device had approximately 1 % efficiency (Shahabuddin, 2024). In the following years, Moser introduced the concept of dye sensitization (Mohsen *et al.*, 2021) by using erythrosine dye on silver halide electrodes. Albert Einstein then elucidated the photoelectric effect in 1905, wherein he secured the Nobel prize in physics in 1921 (Friedman, 2022).

In 1940, Russel Ohi first discovered the n-junction solar cell, which was made from silicon crystalline (Fan *et al.*, 2019). In the 1950s photovoltaic devices were developed using crystalline silicon (Fryer, 2018). In 1954, the first silicon solar cell reported by Chapin achieved an efficiency of 6 % (Shahabuddin, 2024). Furthermore, in 1954, cadmium sulfide was used in a p-n junction photovoltaic device (Kapadnis *et al.*, 2020). Several years after studies on indium phosphide, cadmium telluride, and gallium arsenide, the initial utilization of TiO_2 as a semiconductor in a dye-sensitized solar cell was in the USA (Dey, 2021), and this was reported in a patent in 1978. This cell was based on dye sensitization of anatase TiO_2 nanoparticles with an n-methylphenazinium dye (Zaman & Ahmad, 2022). However, dye-sensitized solar cells remained unsuccessful until the 1990s (Wu *et al.*, 2017). Then in 1991, O'Regan and Gratzel

reported intense power conversion efficiency dye-sensitized solar cell using nanoparticle titanium oxide as the semiconductor electrode sensitized with a ruthenium (bipyridyl) complex dye and using an iodine-iodide electrolyte (Korir *et al.*, 2024).

Ruthenium-based metal complexes dyes are known to have a high carbon footprint because of the complicated chemical synthesis, energy use, and burning of rare metal complexes leading to production of harmful gases which are harmful to the environment (Kaliramna *et al.*, 2022). In contrast, natural dyes obtained from plants sources are harmless to the environment, decompose easily, and require simple synthesis processes (Ragab *et al.*, 2022). Whereas ruthenium-based dyes achieve a higher PCE when used as DSSC sensitizer, natural dyes offer a more sustainable option (Mariotti *et al.*, 2020).

Natural DSSCs present unique benefits at the end-of-life phase. These dyes disintegrate more easily, causing limited environmental harm in the course of disposal. Recycling TCO glass and TiO2 PAs can be reused through recycling. However, some difficulties exist in being able to effectively recycle these elements and materials without compromising performance. The LCA of the natural dyes based DSSCs indicate that despite their reduced PCEs when compared to the ruthenium based counterparts, they provide sustainable alternatives and a fine prospect towards production of environmentally friendly DSSC. (Coppola *et al.*, 2023).

The total amount of greenhouse gases released into the air by mining of raw material, synthesis, and manufacture of a solar cell is called carbon footprint. Dyes of second-generation Ruthenium are widely used as sensitizers in the development of DSSCs due to their better performance and stability. Nevertheless, their fabrication entails energy consuming chemical processes, routinely using materials and synthesis processes that participate substantially in the emission of pollutant gases. As opposed to natural dyes, ruthenium-based dyes predominantly hold a greater carbon footprint. Natural dyes are renewable, biodegradable, and involve simpler extraction processes, presenting a lower clear-cut environmental footprint (Vinoth Kumar *et al.*, 2021). Natural dyes typically result in a lower PCE and short DSSC longevity, that can counteract some of their environmental benefits upon assessed per power output. Therefore, even though ruthenium-based dyes are resource demanding, their high performance could lessen the total carbon footprint. On the other hand, natural dyes provide sustainability gains but need optimization to align with the energy output of ruthenium-base dye systems.

2.2 Dye-sensitized solar cells (DSSCs)

Dye-sensitized Solar Cells (DSSCs) gained their historical roots during the 19th century (Alim *et al.*, 2022). Vogel became the author of the first semiconductor sensitization account

when he used dyes to adjust silver halide emulsion photosensitivity towards infrared wavelengths in 1873, according to Oladepo *et al*. (2022). Moser developed the practice of dye improvement from photographic applications to photovoltaic cells by utilizing erythrosine dye with silver halide electrodes in photo electrochemical cells in 1887 (Tian *et al*., 2019). The theoretical understanding of dye-sensitization faced doubts from 1960 until scientists explicitly established electron transfer as the operational mechanism. The process of electron injection received confirmation from Tributsch and Gerischer when they conducted their research on ZnO in 1968 (Chaudhari *et al.*, 2024). Researchers failed to develop DSSCS because they applied the product to semiconductor surfaces that did not have rough features. Matsumura *et al.*, (1980) presented their findings about energy conversion efficiency at 2.5 % while using sintered porous ZnO disks at 562 nm wavelength. The development of DSSC devices with 7 % efficiency was achieved in 1991 when Gratzel and his team used mesoporous TiO_2, which provided excellent internal surface area (Joseph *et al.*, 2020).

The advancement following these years involved the improvement of semiconductor surface dye adsorption methods, together with advances in nanotechnology to enhance the interfacial surface area (Sapna Yadav *et al.*, 2023). The combination of TiO_2 electrodes produced optimal results because of their non-hazardous properties, low manufacturing expenses, and existence as a widely accessible compound (Danfá *et al.*, 2021; Kumarage *et al.*, 2023). The best DSSC reported so far has realized a conversion efficiency of 12.3 % by co-sensitizing zinc porphyrin dye (YD2-o-C8) with (Y123) dye using a tris (bipyridyl) based redox electrolyte. In addition, the advantages of DSSCs are that they show efficiency increases with temperature from 20°C-60°C and are less affected by fringe light silicon cells (Agrawal *et al.*, 2022; Chen *et al.*, 2007; Kumar *et al.*, 2020). In addition, natural dyes have been developed that produce an efficiency of 2 % to 4 % (Ossai *et al.*, 2021) Synthetic dyes have been studied for many years to produce longer dye excitation lifetimes, strong light absorption in the visible spectrum, and efficient metal-to-ligand charge transfer for ruthenium dyes (Abdellah, 2025; Pashaei *et al.*, 2016). Metal-free organic dyes have been experimented on as sensitizers for DSSCs which include merocyanine, hemicyanine, cyanine, coumarin, perylene, indoline, oligothiophene, dialkylamine dyes, and triphenylamine dyes (Chen *et al.*, 2023; Nalzala Thomas *et al.*, 2021).

2.2.1 Structure and operating principles of the dye-sensitized solar cells

DSSC consists of different fundamental components including a photo-anode (PA) (Alhaji Abubakar *et al.*, 2025), a dye sensitizer adsorbed on the semiconductor, mostly titanium

dioxide (TiO_2), an electrolyte containing a redox couple such as tri-iodide/iodide ions, and a counter electrode (CE) (M Atia *et al.*, 2025), predominantly platinum-coated Fluorine- doped Tin Oxide (FTO) glass (Bandara *et al.*, 2024). The photo-anode consists of semiconductor nanoparticles of titanium dioxide (TiO_2) coated on FTO as depicted in Figure 2.1 (a) (Yadav *et al*., 2020).

These components work in tandem to convert solar energy to electricity (Malumi *et al.*, 2023). During DSSC operates, as shown in Figure 2.1 (b), an incident photon from the sun is absorbed by the dye adsorbed on the surface of TiO_2 film (Domenici *et al.*, 2025). The dye is excited by the incident photon from its ground state (D) to an excited state (D*) (Rxn 1). At this stage, the excited dye has an electron promoted to a higher energy state and then injected into the conduction band of the semiconductor, leaving the dye molecule in an oxidized state (D^+) (Rxn 2) (Kumar *et al*., 2020). The injected electron moves through the TiO_2 film to arrive at the FTO on the PA and then travels across the external circuit to the CE (Rxn 3). At the counter electrode, the electron reduces tri-iodide (I_3^-) in the electrolyte to iodide (I^-) (Rxn 4), which then diffuses into the pores of the TiO_2 film to reduce the oxidized dye (D^+) back to its original state (D) (Rxn 5). This completes the cycle, enabling continuous functioning of the cell. These steps jointly bring about the generation of electrical power.

$$D + h\nu \rightarrow D^* \qquad \text{Rxn 1}$$

$$D^* \rightarrow D^+ + e^- \ (TiO_2) \qquad \text{Rxn 2}$$

$$e^-_{(TiO2)} \rightarrow FTO \rightarrow External\ Circuit \rightarrow \text{CE} \qquad \text{Rxn 3}$$

$$I_3^- + 2e^-_{(CE)} \rightarrow 3I^- \qquad \text{Rxn 4}$$

$$D^+ + 3I^- \rightarrow D + I_3^- \qquad \text{Rxn 5}$$

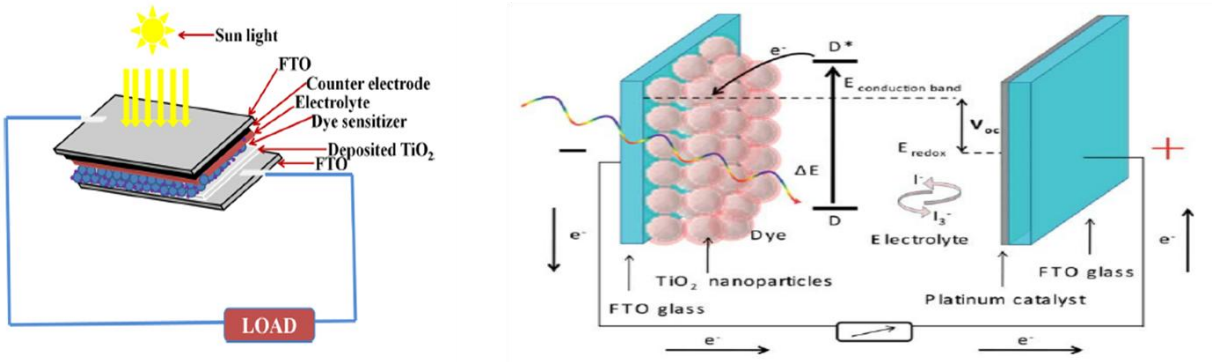

Figure 2.1: (a) Structure of DSSC (b) Operational principles of DSSC

Sources: Calogero *et al*. (2011); Onah *et al*. (2021)

2.3 DSSC's performance parameters

The functioning of DSSC is tested by examining its distinct parameters, including but not limited to the fill factor (Belmahdi, 2025), open-circuit voltage, short-circuit current density, maximum current and voltage, and power conversion efficiency (Huang *et al.*, 2024). Typically, these parameters are examined through the analysis of the current density-voltage (J-V) curves, as depicted in Figure 2.2.

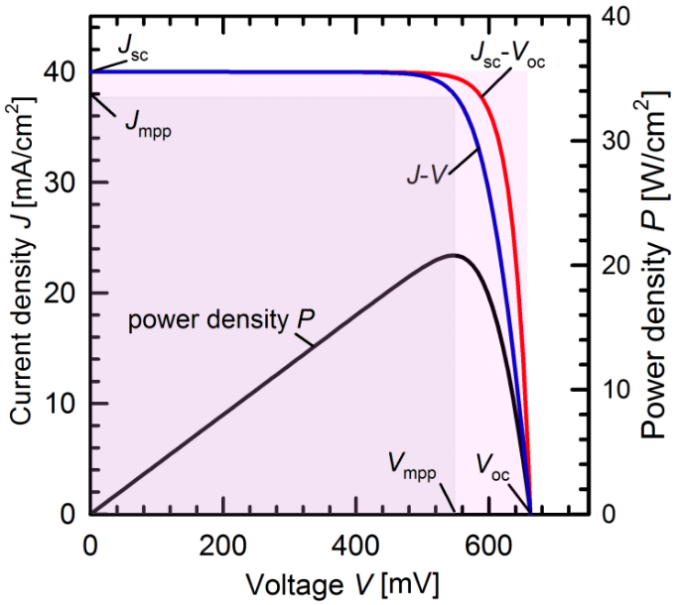

Figure 2.2: DSSC J-V curve

Source: Jain (2020)

The open circuit voltage (V_{OC}) of a solar cell is the voltage across its terminals when there is no external load connected to it (Adak & Cangi, 2024). This is the maximum achievable voltage and is influenced by temperature and light intensity. V_{OC} can also be defined as the

energy difference between the Fermi level of the metal oxide and the redox potential in the electrolyte (Elnemr *et al.*, 2023). The V_{OC} is impacted by the electron affinity of metal oxide and the ionization potential of dye. Raising the energy level of the metal oxide conduction band should reduce the recombination losses and result in a high open-circuit voltage. The suppression of dark current at the metal oxide/electrolyte interface will increase the V_{OC}.

The fill factor (FF) is the ratio of the maximum electrical power (P_m) to the product of short-circuit current and open-circuit voltage, as seen in equation 2.1 (Kataria & Mehta, 2022). It shows the ratio of the useful power to the ideal power produced when all physical conditions are perfect. For example, if the solar power output is 60 W and the ideal power is 100 W, FF of the cell becomes 60 %. FF is associated with the functioning of the interface between TiO_2 semiconductor and redox electrolyte. After absorption of photons from the sun, excited dye is supposed to inject electrons into the conduction band of TiO_2 without allowing recombination, hence high FF. A solar cell can have poor absorbance but higher FF as it only relies on how efficient the electrons are injected into the semiconductor.

$$FF = \frac{P_{mpp}}{I_{SC} \cdot V_{OC}} \tag{2.1}$$

A solar cell can produce current when no load is connected across its terminals (Srivastava *et al.*, 2025). This current is called short-circuit current density (J_{SC}), which is the ratio of the short-circuit current to the exposed surface area (SA) of the cell, expressed as equation 2.2 (Gao *et al.*, 2019). J_{SC} relies on the charge injection and transport (Lee *et al.*, 2025). To achieve a larger J_{SC}, the ejection of electrons must be faster than the reaction with molecules in the electrolyte. As a result, the J_{SC} relies on the performance of the interface of oxide, dye, and electrolyte.

$$J_{sc} = \frac{I_{sc}}{SA} \tag{2.2}$$

The power conversion efficiency (PCE) (Equation 2.3) is defined as the ratio of power produced by the cell (P_{mpp}) to the solar radiation intensity (P_{light}) (Amogne *et al.*, 2020). Maximum charge injection and minimum recombination are the keys to achieving higher efficiency (Shah *et al.*, 2023).

$$PCE = \frac{P_{mpp}}{P_{light}} \tag{2.3}$$

2.4 Photoanode

2.4.1 Substrates

Transparent Conductive Oxide (TCO) substrates form the base for developing the photoanode and counter electrode (CE) in DSSC (Chavan *et al.*, 2023). They provide structural

support for the TiO_2 nanoparticles and the CE catalyst (Kumar *et al*., 2020). TCOs prove invaluable in DSSCs due to their remarkable features such as exceptional chemical and mechanical stability (Kwaśnicki *et al.*, 2024), high optical transparency, an optical band gap surpassing 3 eV, and elevated electrical conductivity (Habis *et al.*, 2022). Indium-tin oxide (ITO) stands out as the most utilized and researched TCO. However, it faces challenges due to limited thermal stability, coupled with the scarcity and toxicity of indium (Qurratulain *et al.*, 2025). As a response, Fluorine-doped tin oxide (FTO) is a favourable alternative to ITO. FTO-coated glass substrates exhibit a wide energy band gap, cost-effective production, thermal stability, and low sheet resistance (Pinheiro *et al.*, 2023).

Sima *et al*. (2010) analyzed FTO and ITO substrates during DSSC fabrication and found better performance in FTO-based cells with 9.6 % PCE, while ITO-based cells had only 2.24 % PCE. They linked the decline in DSSC performance to the high sheet resistance of ITO after annealing at 450 °C. The resistance levels of FTO remained constant throughout the identical heat processing phase. They recommended FTO because of its excellent thermal durability combined with its affordable.

According to Ices *et al*. (2020), both ITO and FTO are high spectrum transparent in the range of UV to visible wavelengths and, therefore, can be used in DSSC applications. ITO electrical resistance begins with 10 Ω -20 Ω values but the values vary considerably with temperature, not the case with FTO. Ruba et al. (2021) investigated electrical resistance of ITO, which is unpredictable during the heat treatments despite the positive visible light absorption. It is proved that FTO is more thermostable with their long-term performance in the temperature range of 550 o C and the cost-effectiveness therefore making it a perfect candidate in the fabrication of DSSC.

2.4.2 Semiconductor

Mesoporous semiconductors accept the injected electrons from excited pigments and transport them to transparent conductive oxide (Yang *et al.*, 2023). The semiconductors employed in DSSCs must boast a large surface area, porosity, and a wide band gap (Arka *et al.*, 2021). Various semiconductor materials have undergone extensive testing for DSSC applications. These materials encompass titanium dioxide (TiO_2), zinc oxide, and zinc stannate. The distinctive optoelectronic characteristics of TiO_2, such as its high dielectric constant and elevated refractive index, cost-effectiveness, and a band-gap of 3.2 eV, position it as a promising material for its application in DSSCs (Orona-Navar *et al.*, 2021).

Dhamodharan *et al.* (2021) researched on the photovoltaic performance of DSSCs based on Indium Tin Oxide (ITO) substrates. The SEM analysis of ITO showed a porous morphology that resulted in PCE of 1.09 %. The preparation of dye adsorbed FTO glass substrate involved preparing a TiO_2 layer through ethanol dispersal (15.0 mL) of 3.5 g of anatase TiO_2 nanoparticles according to Javed *et al.* (2021). After extracting dye from shea nut leaves and adsorbing it on the semiconductor film the efficiency of fabricated DSSC reached 0.25 %. Sarwar *et al.* (2023) performed research comparing DSSC performance between TiO_2 and ZnO semiconductors by testing five different dyes for each material. When tested, both TiO_2 showed better results than ZnO obtained in photoelectric performance. The testing yielded 1.10% photoelectric efficiency through Solanum melongena (eggplant) dye with TiO_2, while ZnO reached only 0.67 %. Better binding of dye molecules with TiO_2 resulted in this distinction in performance.

The research by Sinha *et al.* (2019) analyzed DSSCS that utilized chlorophyll-based dyes for TiO_2 and ZnO metal oxide semiconductors because these dyes display stability on such materials. Under identical experimental conditions, efficiency reached 0.27 % for TiO_2-based DSSCs while ZnO-based devices only reached 0.13 %. Hosseinnezhad *et al.* (2020) pointed out the nanomaterial type is significant in determining DSSC efficiency levels. The study demonstrated that TiO_2 cells exceeded their corresponding ZnO cells in all performance measurements using six different dyes. A single dye designed from TiO_2 achieved a PCE of 12.5 % efficiency as opposed to 7.5 % when fabricated with ZnO.

2.4.3 Dye sensitizers

Dye molecules known as sensitizers fulfill a crucial function when used in dye-sensitized solar cells (DSSCs). Light absorption and electron transfer occur through the dye sensitizer which stands among the most essential components in DSSCs (Omar *et al.*, 2020). An ideal photosensitizer for DSSCs must conform with various important aspects. It should have a high molar absorption coefficient performance in both the visible and near-infrared solar spectrum range (Pirdaus *et al.*, 2024). The presence of carboxylic or hydroxyl anchoring groups enables the formation of a durable connection between dye and semiconductor which ultimately facilitates efficient electron transfer from dye to semiconductor's conduction band. An effective mechanism allows electrons to transfer to the semiconductor more rapidly than the dye's natural degradation. Finally, must maintain photo and thermal stability to avert its degradation and remain inert to avoid side reactions with the electrolyte for a minimum of 20 years (Jabeen *et al*., 2025). Intensive research into dye efficiency improvement, as well as new

sensitizer dye classes, has emerged because of their critical nature. The following are types of dye sensitizers:

i. Ruthenium-based dyes

The benchmark in DSSCs remains established with Ruthenium (Ru)-based complexes, Modified N3 with tetrabutylammonium (N719) and cis-dithiocyanato-bis(bipyridyl)Ru(II) (N3), along with black dye, shown in Figure 2.3 (Fetouh *et al.*, 2024). Ruthenium-based dyes serve as the reference standard in dye-sensitized solar cells because they excel with superior photovoltaic performance along with extensive spectral absorption and persistently stable characteristics. The research conducted by O'Regan and Grätzel since the early 1990s has led to ruthenium complexes becoming essential building blocks for DSSC advancement. N3 dye was later synthesized by combining ruthenium bipyridyl complex components to make a highly effective light-harvesting material for titanium dioxide TiO_2 electron injection (Mauri *et al.*, 2021).

The successful development of the N719 derivative resulted from modifying N3 by substituting its proton with a tetrabutylammonium cation, which created superior organic solvent compatibility combined with easier manufacturing processes (Najm *et al.*, 2023). The black dye ($[Ru(tcterpy)(NCS)_3]$) obtained from ruthenium dyes expanded the absorption spectrum into the red wavelengths to boost the photocurrent output. Ruthenium dyes achieve efficient photo conversions because their strong metal-to-ligand charge transfer processes allow absorption throughout the visible region of the solar spectrum (Abdellah, 2025). The dyes show superior electron injection properties along with slow recombination rates and stable chemical behavior under different conditions. Standard testing conditions have enabled ruthenium dye-based DSSCs to reach power conversion efficiencies of over 30 % (Aghazada & Nazeeruddin, 2018). The application limitations of ruthenium compounds result from production expenses combined with restricted availability of ruthenium complicated synthesis requirements, and weak far-red to near-infrared absorbency. The search for replacement materials became necessary because these compounds remain both expensive and rare while posing environmental dangers (Gupta & Mishra, 2020).

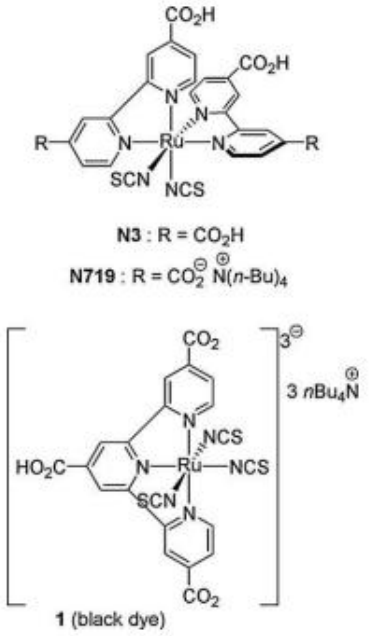

Figure 2.3: Molecular structures of ruthenium (II) dyes N3, N719 and black dye.

ii. Metal-free organic dyes

Metal-free organic dyes have gained interest as dye sensitizers because of their adaptable structures and high light absorption properties (Błaszczyk, 2018). The donor–π–acceptor (D–π–A) design and architecture increase the efficiency of intramolecular charge transfer in these dyes (Li *et al.*, 2021). The literature demonstrates a wide range of organic dyes that achieve efficiency levels beyond 10 % through triphenylamine derivatives, along with indoline compounds and porphyrin derivatives (Periyasamy *et al.*, 2024).

The technology of solar cells has changed to metal-free organic dyes as an alternative to ruthenium-based dyes since they have provided better functionality without raising their cost and environmental sustainability and with ease of making molecular structure changes (Korir *et al*., 2024). They are not metal sensitizers since they have carbons in addition to hydrogen and nitrogen and oxygen elements as an acceptor-donor (D -pi) molecular structure. Another unique geometry in these molecules can facilitate charge transfer between nearby components and be highly absorptive through the visible spectrum and efficient in transferring electrons into the conductive band of the semiconductor (Keremane *et al.*, 2020). Organic dyes excel at high molar extinction coefficient performance that leads to light-absorbing capabilities through thin photoanodes, thus reducing electron recombination while boosting device efficiency (Arunkumar & Anbarasan, 2023).

Scientists have directed their recent energy toward developing modified dye structures that minimize self-aggregation while enhancing stability and improving energy level compatibility

with semiconductor materials, along with redox electrolytes (Nalzala Thomas *et al*., 2021). Power conversion efficiencies get improved through the combined usage of dyes, which have different absorption spectra that match each other in a co-sensitization method. Research explores integrating metal-free dye systems with either cobalt or copper-based redox shuttles because these systems produce an enhanced open-circuit voltage (Masud & Kim, 2023).

iii. Natural dyes

Plant pigments are distinctive compounds that possess the ability to absorb various wavelengths of light, resulting in vibrant colors (Acquavia *et al*., 2021). These pigments act as signals, drawing in insects, birds, and animals to aid in pollination and seed dispersal (Gahlawat, 2019). The main plant pigments include carotenoids, flavonoids, and anthocyanins. These pigments have powerful antioxidant activities and multiple health benefits (Lu *et al.*, 2021). Apart from carotenoids, chlorophylls (molar mass 893.5 g/mol), anthocyanin (449.2 g/mol), and betanin (550.5 g/mol) are crucial for photosynthesis (Sun *et al*., 2023). In the photosynthetic process, carotenoids serve as auxiliary pigments for light harvesting (Semalti & Sharma, 2020). They also protect the photosynthetic apparatus from possible harm brought on by intense light (Zulfiqar *et al*., 2021). Natural dyes from various plant sources, including fruits, vegetables, flowers, seeds, roots, or leaves, have been used as photosensitizers in DSSCs due to their ready availability, inexpensive, and eco-friendly.

Natural dyes should be considered as a replacement for ruthenium-based dyes as they are; eco-friendly and readily available minimizing reliance on expensive ruthenium-based metal complexes. Organic dyes are biodegradable and present no environmental adverse effect, making them viable substitutes (Roslan *et al.*, 2018).

iv. Porphyrin-based dyes

Porphyrins act as artificial alternatives to natural pigments, which capture optical energy. The application of molecular design principles in recent times has achieved remarkable improvements in both the light absorption and electron transfer abilities of these materials (Park *et al.*, 2021). The optimized configuration of DSSC cells using YD2-o-C8 reaches performance efficiencies greater than 12 %. Dye-sensitized solar cells (DSSCs) depend primarily on Porphyrin-based dyes as sensitizers because they exhibit excellent light-harvesting capabilities as well as high chemical stability, together with their structure that resembles chlorophyll and other natural pigments (Kodji *et al.*, 2025). The dyes possess a wide macrocyclic planar ring that enables their absorption strength to cover both visible and near-infrared solar spectrum frequencies for DSSC photocurrent optimization. These pigments demonstrate suitable

photoactivity by replicating natural photosynthetic activities, which makes them excellent choices for solar energy harvest (Zeng *et al*., 2020).

Initial applications of simple porphyrin dyes in devices did not achieve high degrees of performance due to their very weak attachment to the semiconductor materials as well as to the matching of energy levels. With the aid of molecular engineering, scientists have managed to design asymmetrical structures that have been able to extend π-conjugation systems and incorporating electron donor and electron acceptor groups that have increased the efficiency of light absorption and the concentration of electron holes in the substances (Huang *et al*., 2024). The successful YD2-o-C8 dye combines an alkyl chain for aggregation prevention together with a TiO_2-binding carboxylic acid group (Abdullah, 2025). When combined with suitable organic dyes and cobalt redox electrolytes, the porphyrin dye delivers power conversion efficiencies exceeding 12 %, demonstrating its competitive capabilities against ruthenium complex usage in DSSCs (Ji *et al.*, 2018). Like organic dyes, the commonly used porphyrin dyes adopt donor–π–acceptor (D–π–A) structures but engineer the porphyrin core to increase electron donation capability and widen absorption spectral range (Zeng *et al.*, 2020). Electronic binding to the semiconductor occurs with the assistance of cyanoacrylic acid acceptors, and aryl amines or thiophenes donors function as common donor groups. The deliberate modifications increase both the photophysical performance and lower charge recombination and extend the electron lifetime performance of the device (Huang *et al*., 2024).

2.5 Electrolytes

Electrolytes consist of redox compounds capable of electron exchange, facilitating the renewal of the dye (Ikpesu *et al.*, 2020). Common characteristics of electrolytes include excellent ionic conductivity, effective oxidation or reduction of the dye molecule, and non-reactivity with the dye sensitizer (Arka *et al*., 2021). The three main electrolyte types are liquid, quasi-solid, and solid-state (Hwang *et al.*, 2021). Among these, the liquid electrolyte with iodide/tri-iodide redox couple stands out as the most prevalent for DSSCs fabrication (Sen *et al*., 2023).

2.6 Counter electrode

In DSSCs, TCO substrates are coated with a catalyst to form a counter electrode (CE) (Hasan & Susan, 2025). At the CE, the catalytic reduction reaction occurs, facilitating the flow of electrons from an external circuit to reach the electrolyte (Meyer *et al.*, 2018). The essential characteristics required for an effective CE include high catalytic activity, low charge transfer resistance, and an improved exchange current density (Arka *et al*., 2021). Carbon-based

materials, conducting polymers, alloys, and transition metal compounds have emerged as crucial catalysts for CEs (Kharboot *et al.*, 2023). Among these options, platinum serves as a superior catalyst, with notably high electrical conductivity (Khajavian *et al*., 2020).

2.7 Chemical structure of natural dyes

Scientific research has examined different plant-sourced materials for use in DSSC devices (Amogne *et al*., 2020). Plants contain water-soluble flavonoids named anthocyanins, which are found in different fruits and vegetables (Mattioli *et al*., 2020). Betalains, together with carotenoids, occur naturally in numerous fruits as well as plants and roots according to Calva-Estrada *et al*. (2022). Plant tissues containing chlorophyll exist in almost every green vegetation (Ebrahimi *et al*., 2023). Betalain pigments, including red betacyanins and yellow betaxanthins, show promising capabilities for solar energy conversion. Betalain pigments encompass potentially useful compounds for solar energy transformation through their red betacyanin and yellow betaxanthin components. Betanin, a type of betacyanin, exhibits a peak absorbance at 535 nm with a molar absorptivity of 65,000 $M^{-1}cm^{-1}$ (Ambedkar & Pradesh, 2019). Table 2.1 depicts the chemical structures of select natural dyes.

Table 2.1: Chemical structure of select natural dyes.

Dye	Chemical structure	Absorption range (nm)	Common Source	Reference
Chlorophyll	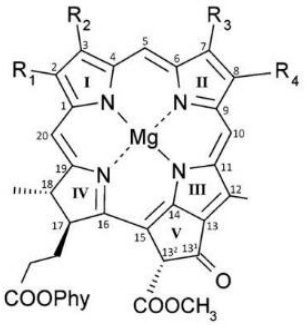	400–420, 650–700	All photosynthetic plants	(Tamiaki, 2022)
Betalains		500-580	Red beetroot, prickly pear fruit, and amaranth	(Gomesh *et al*., 2016)

Name	R_1	R_2	R_3	R_4
Chlorophyll *a*	CH_3	$CH{=}CH_2$	CH_3	CH_2-CH_3
Chlorophyll *b*	CH_3	$CH{=}CH_2$	CHO	CH_2-CH_3
Chlorophyll *d*	CH_3	CHO	CH_3	CH_2-CH_3
Chlorophyll *f*	CHO	$CH{=}CH_2$	CH_3	CH_2-CH_3

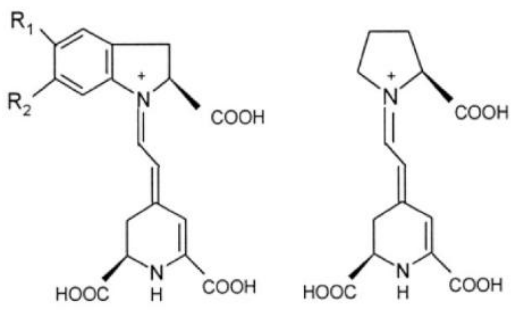

Betacyanins **Indicaxanthin**

Betanidin: R_1 and R_2=OH
Betanin (5-*O*-glucose betanindin): R_1=glucose; R_2=OH

Chlorophyll has a central magnesium ion that bonds to the porphyrin ring system that includes four pyrrole subunits to provide its molecules with their ability to absorb light (Singh & Shukla, 2022). Two varieties of chlorophyll exist as chlorophyll a and chlorophyll b, which vary based on the chemical group found at the carbon position 7: chlorophyll a has a methyl group attachment, and chlorophyll b displays an acetal group (Ikyo *et al*., 2020). Chlorophylls absorb visible light energy through the wavelength range of 420–460 nm in blue wavelengths and 650–700 nm in the red part of the spectrum, while emitting reflective green wavelengths that give plants their green color (Khammee *et al*., 2021).

Among the various types of pigments found within flavonoids, anthocyanin stands out as the most prevalent. In flowers, the most frequently encountered anthocyanidins include pelargonidin, cyanidin, delphinidin, petunidin, and malvidin (Jaafar *et al.*, 2018). Carbonyl and hydroxyl groups in anthocyanin molecules are connected to the semiconductor TiO_2 surface, enabling the transfer of electrons (Patni *et al.*, 2020). Anthocyanin pigments display their maximum absorption spectrum between 500-535 nm (Bernardi *et al.*, 2019).

2.8 Natural dye co-sensitization

The majority of solar radiation that reaches the Earth's surface falls within the wavelength range of (300–2600) nm (Cachorro *et al.*, 2021). This encompasses ultraviolet (UV) (<380 nm), visible (380–780) nm, and near-infrared (NIR) light (>780 nm). The solar spectrum comprises (3–5) % UV, (42–43) % visible, and (52–55) % NIR light (Wang & Yu, 2023). To enhance the efficiency of a solar cell, the absorption of photons within the visible region needs to be optimized (Lee *et al.*, 2018). Co-sensitization emerges as a crucial strategy for elevating the efficiency of DSSCs by augmenting their capacity to absorb light (Krisha *et al*., 2017). Co-sensitization serves to mitigate recombination kinetics (Hupfer *et al.*, 2025), thereby enhancing the current output and cell efficiency (Soosairaj *et al*., 2023). Co-sensitization of natural dyes for application in DSSCs has been heavily reviewed in the published literature, as enumerated in Table 2.2.

Chlorophyll, anthocyanin and betanin natural dyes have distinct UV-vis absorption characteristics which render their capacity to absorb light. Light is mainly absorbed during two wavelength ranges of 430 -450 and 660 -680 in Chlorophyll. Anthocyanins present strong peaks in the region of 500–550 nm, while betanin displays a conspicuous absorption peak around 535–540 nm. Figure (2.4), (2.5), and (2.6) show the absorption spectra of chlorophyll, anthocyanin, and betanin.

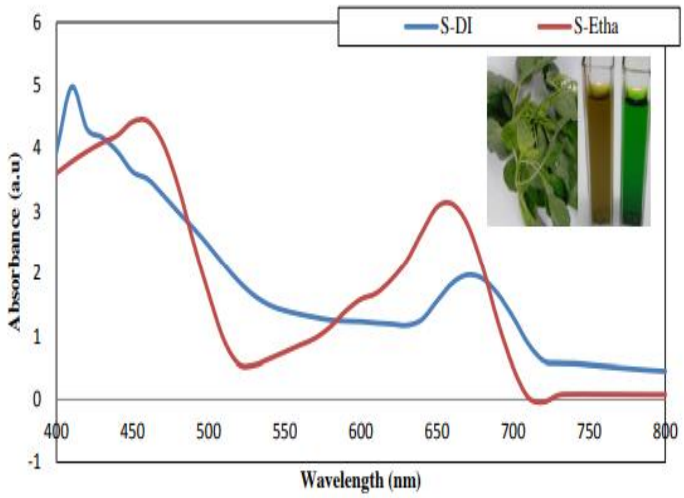

Figure 2.4: Chlorophyl UV-Vis absorption spectrum (S-Etha and S-DI) (Syafinar *et al.*, 2015).

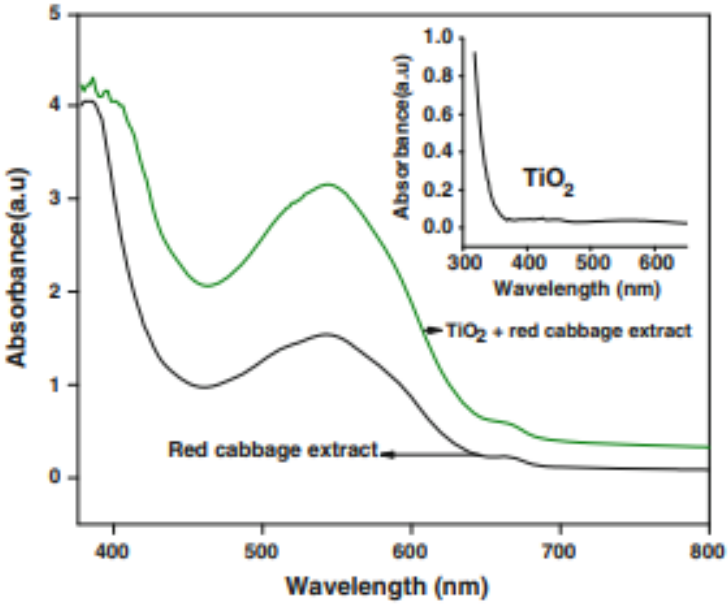

Figure 2.5: Anthocyanin UV-Vis absorption spectrum (Gokilamani *et al.*, 2013).

Table 2.2: Photovoltaic parameters of single-sensitized and co-sensitized DSSCs.

	Natural dye	Source	Extracting solvent	J_{SC} (mA/cm^2)	V_{OC} (mV)	FF (%)	PCE (%)	Reference
1	Chlorophyll	*Talinum fruticosum*	Ethanol at 65°C	0.65	560	0.49	0.18	(Ezike *et al.*, 2021a)
	Anthocyanin	*Caesalpinia pulcherrima*		0.74	710	0.48	0.25	
	Co-sensitized			2.91	640	0.61	1.14	
2	Betanin	red beetroot	Acidified ethanol	1.00	530	0.646	0.562	(Sreeja *et al.*, 2018)
	Chlorophyll-a	Spinach	Absolute ethanol	0.11	530	0.722	0.047	
	Co-sensitized			1.25	503	0.680	0.601	
3	Chlorophyll	*Malva verticillate*	Microwave-assisted extraction	5.68	540	55.4	1.70	(Golshan *et al.*, 2021)
	Anthocyanin	*Syzygium cumini*	(pure ethanol)	5.16	200	26.1	0.27	
	Co-sensitized			2.12	0.39	37.2	1.84	
4	Betalain	O. dilleniid	Methanol and HCl (99:1)	6.81	521	0.69	0.47	(Teja *et al.*, 2023)
	Anthocyanin	T. indica		2.19	532	0.67	0.14	
	Co-sensitized			3.17	529	0.64	0.20	

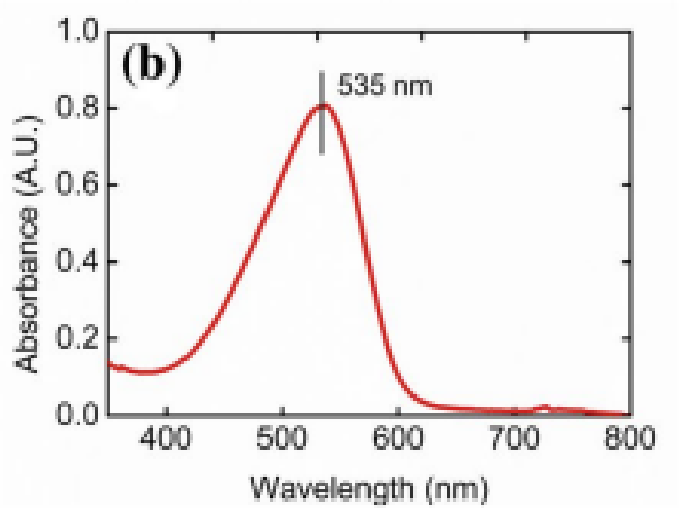

Figure 2.6: UV-Vis absorption spectrum for betanin (Sreeja & Pesala, 2018).

2.9 Annealing temperature

The overall output of dye-sensitized solar cells (DSSCs) relies on the annealing temperature during titanium dioxide (TiO_2) photoanode fabrication because this process controls both the crystalline structure and properties of TiO_2 films (Awsha *et al.*, 2021), together with their surface characteristics and electrical behavior (Ansir *et al.*, 2021). The anatase phase emerges at 400–500 °C during annealing to produce crystalline TiO_2, which makes electron transport efficient because of its exceptional photocatalytic properties (Onah *et al.*, 2021). The electron injection efficiency of TiO_2 suffers from annealing treatments exceeding 600 °C since the process leads to anatase-rutile phase transformation that produces a material with a lower conduction band edge.

The utilization of TiO_2 films that undergo annealing above 600 °C results in dominant rutile phase formation, which affects both dye absorption ability and electron movement, thus causing cell performance degradation (Muthee & Dejene, 2021). Annealing affects the morphology of TiO_2 films through modifications of their crystallinity but mainly by altering their grain dimensions and surface exposure area (Hakki *et al.*, 2018). The increase in annealing temperature brings about grain enlargement thus diminishing the accessible area for dye absorption. The annealing process controls how TiO_2 films conduct electricity (Blanco *et al.*, 2018). Heat treatments at 450 °C result in superior electron mobility (Chen *et al.*, 2025) with extended lifetimes attributed to lower defects in the material but higher temperatures cause electron recombination via combined effects of film expansion and structural damage to the

material (Bist & Chatterjee, 2021). The duration of annealing contributes equally to device performance (Gu *et al.*, 2024). The device efficiency and crystallinity improve with extended annealing time up to a certain point, but efficiency starts decreasing due to abnormal grain growth. Research has investigated complex annealing methods as well as profiles for improving TiO_2 functionality (Zhang *et al.*, 2023). Both annealing temperature and time require exact control to modify TiO_2 photo anodes structurally and electronically to achieve higher efficiency in DSSCs (Syrek *et al*., 2020).

2.10 Dye adsorption time

Dye adsorption time is crucial to the design of dye-sensitized solar cells (DSSCs) since it influences the functionality of the TiO2 photoanode (Yeoh & Chan, 2017). Light efficiency and electron behaviour are altered by the duration of dye exposure, which also affects the number of molecules absorbed on TiO2 surfaces (Reza *et al*., 2017). (Hossain et al., 2018). Research has indicated that the ideal duration for dye adsorption on TiO2 photoanodes creates a monolayer that enhances dye loading and charge injection efficiency (Jagtap *et al*., 2021), resulting in a more significant short-circuit current density (JSC) and power conversion efficiency (PCE) (Jagtap *et al*., 2021). It has been proven that extending the time of dye soak leads to better attachment of dye molecules on TiO_2 surfaces, which results in higher optical absorption and elevated electron injection rates (Kandregula *et al*., 2025). The process of dye aggregation becomes more severe when adsorption times extend beyond optimal lengths, thus inhibiting electron transport while increasing recombination reactions that degrade device performance (Xu *et al*., 2020).

The dye molecules take longer time to enter the porous structures when the thickness of the film is more than some limits. The short adsorption times are not normally necessary to achieve maximum dye loading in TiO2 films the reason is that the TiO2 films generate an under adsorbed photoanode resulting in fewer photons being absorbed and a reduction in JSC. The performance of DSSC involves the adequate use of dye adsorption times depending on the chosen film thickness (Ruhane *et al.*, 2017). The chemical stability of semiconductor materials determines the appropriate dye adsorption periods because it affects the overall process (Shweta Yadav *et al.*, 2023). The chemical stability of TiO_2 exceeds that of ZnO and other semiconductors, which enables longer dye immersion duration without major structural degradation (Boro *et al.*, 2018).

2.11 Spectrophotometry and the Beer-Lambert law

UV-VIS spectrophotometry is a method for measuring light intensity absorbed by a sample in the ultraviolet (180-380) nm (Li *et al.*, 2024) and visible light (380-780) nm wavelengths (Pratiwi & Nandiyanto, 2022). The quantity of radiation absorbed by the analyte is determined by how much of a certain wavelength of light it absorbs (Mulya Harahap *et al.*, 2025). It forms the basis for analyzing a variety of substances, including organic, inorganic, biological, and pharmaceutical compounds (Sudharshan & Swetha, 2023). A chromophore, found within a molecule, is responsible for giving it its color (Bera *et al.*, 2020). This color is visible when the molecule absorbs particular wavelengths and reflects others. The reflected light then exhibits a complementary color to the absorbed light wavelengths (Chen *et al.*, 2024).

The complementary colors are positioned opposite each other (Awad *et al.*, 2025). Consequently, the absorption of violet light wavelength imparts a yellow color to a substance (Das *et al.*, 2024), while the absorption of red light wavelength results in a green color. The Beer-Lambert law asserts that the concentration of a solution is directly linked to the absorbance of light (Wathudura *et al.*, 2025), which is depicted by Equation (2.4) (Zainurin *et al*., 2023). Here, A_λ is the absorbance of the sample at a specific wavelength, ε is the molar extinction coefficient, c is the concentration of the solution, and *l* is the thickness of the cuvette (Delgado, 2022).

$$A_\lambda = \varepsilon c l \tag{2.4}$$

CHAPTER THREE
MATERIALS AND METHODS

3.1 Materials and equipment

The materials used in designing DSSCs for this study included diverse components: Fluorine-doped tin oxide (FTO) coated glass slide 2.00 cm x 1.50 cm x 0.22 cm having a surface resistivity of 7 Ω/sq. Anatase TiO_2 nano-powder, 21 nm primary particle size. Fresh *Spinacia oleracea* leaves, *Beta vulgaris* tubers, and *Rubus fruticosus* fruits used in this research are depicted in Figure 3.1 and were acquired after consulting with specialists from the agricultural and botanical departments, at Egerton University. This team of specialists offered crucial pieces of advice and was available for consultations.

Figure 3.1: Raw materials for dye extraction

In this study, Iodolyte AN-50 electrolyte was used, formulated with acetonitrile as the solvent. The platinum catalyst was prepared from hexachloroplatinic (IV) acid hexahydrate (PanReac AppliChem). Other materials included: ethylene glycol, potassium iodide, ethanol, methanol, acetone, iodide, isopropanol, and titanium (IV) tetraisopropoxide. Apparatus utilized included Petri dishes, beakers, test tubes, a mortar and pestle, an electronic weighing scale, a magnetic stirrer, a multimeter, a fine sieve, a blender, and a hot plate. For characterization purposes, the following equipment were employed: Fourier transform infrared spectroscopy, Ultraviolet-Visible (UV-Vis) Spectrophotometer, and a solar cell simulator.

3.2 Cleaning of substrates

Figure 3.2 illustrates the schematic presentation of the FTO substrate cleaning process. Initially, these substrates were rinsed in running water to remove the debris that might be present, followed by ultrasound sonication with detergent and distilled water for 10 minutes. After that, the substrates were cleaned using a cotton ball soaked in acetone and then rinsed in deionized water (DI) in an ultrasonic bath. Finally, the samples were ultrasonicated with acetone for 30 minutes and left to dry. Cleaned substrates were kept in covered petri dishes to

avoid contamination from dust and any other foreign material that may lead to poor adsorption of dyes.

Figure 3.2: FTO Glass substrates cleaning process

3.3 Film deposition

3.3.1 Preparation of TiO_2-coated FTO

Commercial anatase phase of titanium nano-powder was chosen due to its high photocatalytic activity. The TiO_2 film was prepared through a mixture comprising 3.50 g of commercial TiO_2 nano powder and 15.0 mL of ethanol and later sonicated for 30 minutes. Subsequently, ethyl cellulose was added to the suspension and magnetically stirred to form a homogenous solution as binder is dissolved, then evaporate at 60 °C. A multimeter was used to identify the conducting side of FTO glass substrates as shown in Figure 3.3.

Figure 3.3 : A multimeter.

FTO was chosen due to its superior performance under high-heat treatment. Upon identifying the conductive area, the working area was then demarcated using adhesive tape around the sides of the FTO substrate as shown in Figure 3.4.

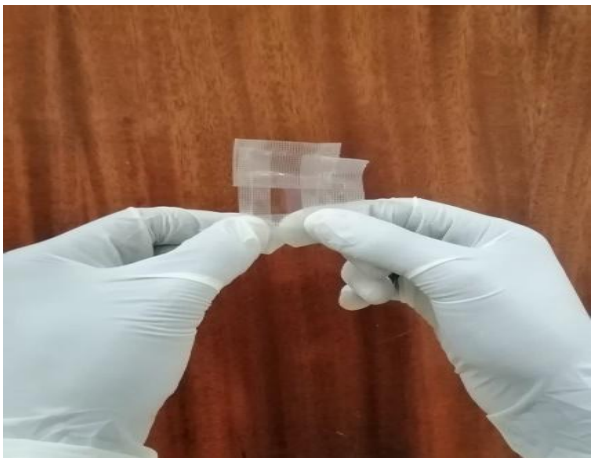

Figure 3.4: Demarcating FTO glass for TiO2 deposition.

The prepared TiO_2 paste was dropped onto the delimited area of FTO glass substrates. Using the doctor's blade method, a glass applicator was used to evenly spread the suspension across the marked area of the substrates, forming a uniform film. The film was left to dry before removing the adhesive tape. Finally, the TiO_2-coated FTO substrates underwent pre-heating at 150 °C for 30 minutes to evaporate ethyl acetate and to prevent cracking that occurs during heating at higher temperatures, followed by cooling. The samples were then annealed at selected temperatures of 250, 350, 450 and 550 °C on a hotplate for 1 h. Annealing was carried out gradually under nitrogen gas to improve crystallinity, relieve internal stress, and enhance the electrical and optical properties of the samples.

3.3.2 Counter electrode preparation

The platinum reductive catalyst was prepared by mixing 1.0 mL of hexachloroplatinic (IV) acid hexahydrate (5 mM) into 207.0 mL anhydrous isopropanol, then stirred at 350 rpm for half an hour. The product was spread on the FTO substrate using a soft brush as shown in Figure 3.5, then underwent sintering at 500 °C for 30 minutes for the constituent materials could fuse.

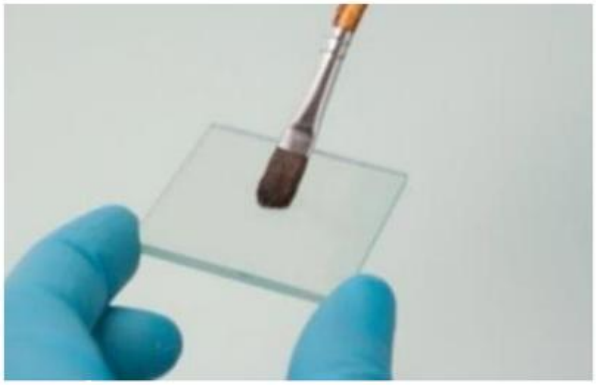

Figure 3.5: Counter electrode coating.

3.4 Extraction of dyes

Dyes were extracted from *Spinacia oleracea* (spinach) leaves (A), *Rubus fruticosus* (blackberry) fruits (B), and *Beta vulgaris* (beetroot) roots (C). Fresh leaves taken from *Spinacea oleracea* in a greenhouse were washed in distilled water to remove residual material. After cutting the leaves into smaller pieces, they were (100 g) kept separately in a blender and blended for 2.0 minutes. Subsequently, the extracts were transferred into separate glass bottles, followed by the addition of ethanol (80 %) which helps in extraction. The mixture was filtered using Whatman filter paper to separate solid material from dye extract. The extract was concentrated using a rotary evaporator, stored in amber bottle and kept in refrigerator at 4.0 ℃ to prevent degradation of chlorophyll.

Fresh tubers of *Beta vulgaris* were first cleaned thoroughly using distilled water to remove dirt and then cut into small pieces to increase the surface area for dye extraction. A 100 g portion of the sliced tubers were placed in a blender and blended for 2.0 minutes. The blended extracts were transferred into a glass bottle, and methanol was added to ease pigment extraction. The mixture was then filtered using filter paper to separate solid residue from dye extract. To achieve high purity, the filtrate was mixed with acidified (hydrochloric acid) methanol to remove unwanted proteins. The dye extract was kept in an amber bottle and then stored in a refrigerator at 4 ℃ to prevent oxidation awaiting characterization.

Fresh ripe *Rubus fruticosus* fruits were first washed with distilled water to remove surface impurities. 100 g of the cleaned fruits were blended with 5 mL acidified (0.1 % HCl v/v) ethanol to stabilize anthocyanin, then stirred for 40 minutes to avoid degradation of anthocyanin pigments. Afterward, the mixture was filtered using Whatman filter paper, and the filtrate was concentrated using a rotary evaporator. The resulting mixture was stored in sealed bottle, covered with aluminum foil, and kept at room temperature overnight for sedimentation

The concentrated extract was then kept in a refrigerator at 4 ℃ to prevent oxidation. The color of extracts is shown in Figure 3.6; deep red (anthocyanin), green (chlorophyll), and deep purple (betanin).

Figure 3.6: Dye extracts.

Dye mixtures were *Spinacia oleracea* + *Rubus fruticosus* (D), *Spinacia oleracea* + *Beta vulgaris* (E), *Rubus fruticosus* + *Beta vulgaris* (F), and *Spinacia oleracea* + *Rubus* fruticosus + Beta *vulgaris* (G) at 1:1 and 1:1:1 volume ratio as shown in Figure 3.7.

Figure 3.7: Dye mixture

3.5 Characterization techniques for dye solution

The characterization techniques employed were critical for validating or refuting the proposed hypotheses, as well as for facilitating comparative analysis of the dye solutions. All measurements were conducted under controlled and contamination-free conditions, guaranteeing consistency and accuracy of the results. Furthermore, given that some of the required instrumentation was housed in external institutions, it was deemed necessary to schedule the experimental procedures every week to accommodate equipment availability and maintain consistency.

3.5.1 Fourier-Transform Infrared (FTIR) spectroscopy

Dye samples were analyzed with an FTIR spectrometer model 8400 at the Chemistry Department at JKUAT University. The cell was prepared by assembling it with IR-transparent windows, typically made of sodium chloride cell (NaCl). A few drops of dye extract liquid samples were introduced into the cell (done separately for each of the seven samples). The cell was properly sealed to prevent leakage, then was mounted on a sample holder for FTIR analysis through the mid-IR region from 4000 cm^{-1} to 400 cm^{-1} to determine the functional groups. The experiments were conducted in triplicate for reliability and accuracy of the data.

3.5.2 UV-Vis spectrophotometry

The potent photovoltaic characteristics of DSSC depend on both the dye's capacity to absorb light and the electron diffusion within the optical window of the material (Rahman *et al*., 2023). UV-Vis absorption spectra depict how pigments absorb solar energy at different wavelengths. To put it differently, it facilitates the identification of the type of wavelength of light that are absorbed and the ones that are transmitted or reflected. Dye solutions in this study included Spinacia *oleracea*, *Beta vulgaris*, and *Rubus fruticosus* and their mixtures *Spinacia oleracea* + *Beta vulgaris*, *Spinacia oleracea* + *Rubus fruticosus*, *Beta vulgaris* + *Rubus fruticosus, and Spinacia oleracea* + *Beta vulgaris* + *Rubus* fruticosus. The optical absorption properties of these dye extracts were studied using a UV-Vis spectrophotometer shown in Figure 3.8.

Figure 3.8: UV-Vis spectrophotometer setup used for absorbance measurement.

After preparing all the seven dye extract solution samples, the cuvette was filled with pure ethanol (without dye) to use as a blank. This blank (reference) is used to correct absorption

from the ethanol (solvent) or any other constituent in the system apart from the dye sample. A different cuvette was filled with the prepared dye solution, ensuring there were no bubbles. The exterior part of the cuvette was wiped dry to remove fingerprints and solvent residue. The blank was placed in the UV-Vis spectrophotometer initially to calibrate it, followed by measurement of the absorbance of the dye solution across the 400-800 nm wavelength range. This procedure is potentially detailed by The Beer Lambert law, expressed in equation 3.1, that links the incoming_light intensity (I_0) on the surface of a cuvette of length, *l*, (cm, usually 1 cm) of an absorbing dye solution of concentration, c (mol·L^{-1}), to the transmitted light intensity (emerging from the cell) by the dye sample (I). ε (L·mol^{-1}·cm^{-1}) is known as the molar absorptivity and is a measure of how strongly the dye sample absorbs light.

$$\log(I_0/I) = -\log(\%\,T/100\,\%) = \varepsilon c l = A_\lambda \quad (3.1)$$

3.6 DSSCs fabrication

Fabrication of DSSCs was done single and mixed dye extracts as sensitizers. TiO_2 films were immersed in dye extracts in a dark place while timing a duration of 20 h, 30 h,40 h and finally 50 h separately. After dye sensitization, the photoanodes were rinsed with ethanol to remove unbounded residues, followed by air drying at room temperature (25 °C), and finally stored in dark place to avoid oxidation with air awaiting cell fabrication. A total of seven DSSCs were successfully fabricated and prepared for subsequent photovoltaic performance characterization. The performance of these dyes was determined from the performance of the photovoltaic parameters of fabricated DSSCs using a solar simulator. The dye extract exhibiting the highest performance was selected for further investigation, specifically to examine the effect of annealing temperature and dye soaking duration on the photovoltaic performance of DSSCs.

3.6.1 Electrolyte preparation

To prepare 0.5 M iodine solution, 200 g of potassium iodide was first dissolved in about 350.0 mL of deionized water. 127 g of iodine (I_2) was then added and stirred using a magnetic stirrer for an hour in a dark environment until all the iodine crystals dissolved to avoid oxidation as seen in Figure 3.9 (Ferreira *et al.*, 2022). The solution was then transferred into a 1000 mL volumetric flask and filled to the mark with deionized water. The solution was finally standardized using sodium thiosulfate. The resulting electrolyte solution was stored in an opaque container away from light exposure.

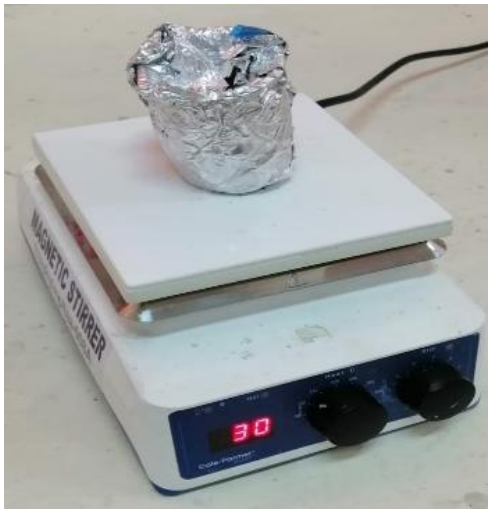

Figure 3.9: Stirring electrolyte using a magnetic stirrer

3.6.2 DSSCs assembling

After the annealing process of TiO_2-coated FTO, the substrates were cooled, immersed in single and mixed dye solutions (Figure 3.10), for different periods of 20, 30, 40, and 50 hours.

Figure 3.10: Sensitizing TiO2-coated glass substrate

The adsorption experiment was performed in a dark environment, with beakers covered with aluminum foil to prevent photo degradation. The photoanodes were subsequently left to dry in air at room temperature (25 ℃) to allow full adsorption of dye molecules onto the TiO_2 surface. The optimal dye loading time is determined by the photovoltaic performance of DSSCs using a solar simulator. The DSSC devices were then assembled by sandwiching dye-coated photoanode and a counter electrode, utilizing the prepared sensitizers and co-sensitizers. The inter-electrode space was then filled with a redox electrolyte to complete the cell structure.

Platinum-coated CE surface and dye-sensitized PA surface of DSSC were affixed facing each other, and the two were secured together using binding clips to avoid electrolyte leakage. Subsequently, a few microliters of a redox electrolyte solution were introduced between the CE and PA dropwise. These electrodes were then connected with conducting wires as depicted in Figure 3.11.

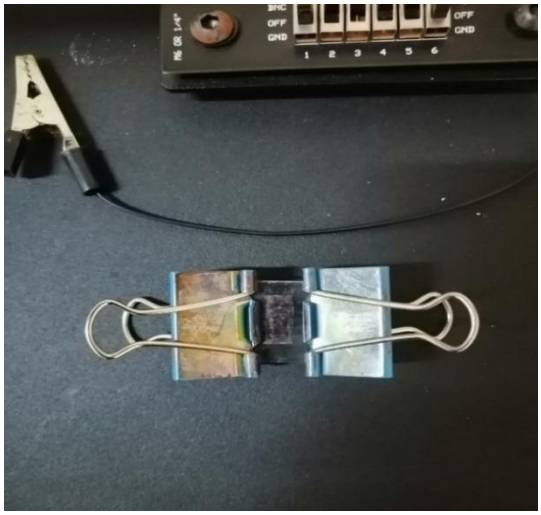

Figure 3.11: Fabricated DSSC

3.7 DSSCs Photovoltaic performance

A solar simulator shown in Figure 3.12 was used to provide a standard solar spectrum, usually AM 1.5 G condition at an irradiance of 100 mW/cm². A masking tape was used to delimit the active area of the DSSC at the time of measurement. The masking tape thwarts scattered light from affecting the cells photovoltaic parameters hence guaranteeing accurate PCE computation. Fabricated DSSC was connected to a source meter using crocodile clips to the exposed conductive part of the photoanode and counter electrode. Photoanode was then exposed to the light source and the software that comes with the solar simulator was used to apply a range of voltages to the cell and the corresponding current densities were read and recorded. The measurements were repeated five times to ensure reliability of the data. Current densities measured were plotted against the voltages and the resulting J-V curves were used to determine photovoltaic parameters. The overall quality and performance of the fabricated DSSCs were determined by the fill factor (FF) and power conversion efficiency (PCE). Electrical characterization was conducted in the Materials Science Laboratory present in the Physics Department, Egerton University.

Figure 3.12: A solar simulator used to test fabricated cell performance

CHAPTER FOUR
RESULTS AND DISCUSSIONS

4.1 Fourier Transform Infrared (FTIR) spectroscopy analysis

An essential requirement for a successful photosensitizer is the existence of specific functional groups attached to the TiO_2 (Al-horaibi *et al.*, 2023). Dyes possess different functional groups for different roles, anchorage, absorption, and electron transport. As part of characterization, this study investigated chemical functional groups contained in the dye extracts using Fourier Transform Infrared (FTIR) spectroscopy by comparing with reference spectra of chlorophyll, anthocyanin and betanin from literature. Figure 4.1 depicts findings within the ranges of 4000-400 cm^{-1}, in which FTIR spectra of the dye extracts obtained from *Spinacia oleracea*, *Rubus fruticosus*, and *Beta vulgaris* are displayed.

The FTIR spectrum of *Rubus fruticosus* extract, illustrated in Figure 4.1(a), reveals a broad band at 3332 cm^{-1}, that is attributed to the stretching vibrations of the hydroxyl (–OH) functional group. Furthermore, C–H stretching vibration at 3016 cm^{-1} and at 1778 cm^{-1} indicate the presence of stretching vibration of the ester carbonyl group (C=O) in confirmation with Chang *et al*. (2013). A band at 1608 cm^{-1} was detected largely because of the C=C double bond stretching vibration. The spectrum also showed a band at 1440 cm^{-1} corresponding to the deformation of C–H bonds (Dhafina *et al.*, 2018). The intense peak at 1012 cm^{-1} was in confirmation with that of the C–O bonds stretching of phenol. The observed absorption bands depict characteristics of functional groups of anthocyanin. These peaks are characteristic of the anthocyanin base molecule, favorably validating the potency of good photosensitization in solar photovoltaics (Jaafar *et al*., 2018)

The FTIR spectrum of the dye extract obtained from *Spinacia oleracea,* as presented in Figure 4.1 (b), reveals a prominent absorption band at 3558 cm^{-1}, which is assigned to the O-H stretching vibration characteristic of hydroxyl functional groups (Patni *et al*., 2020). The peak seen at 2817 cm^{-1}, can be imputed to belong to C-H_2 vibration of aliphatic groups. The C-H stretching broadens widely within the dye extract to deal with the absorption energy (Azlina *et al.*, 2023). Additionally, C=O conjugation groups, C-O vibration, and the C-H bending frequency are seen at 1692 cm^{-1}, 1064 cm^{-1}, and 983 cm^{-1}, respectively, all showing characteristics of the chlorophyll pigments (AM Al-Alwani *et al.*, 2019).

Figure 4.1 (c) shows the FTIR spectrum of *Beta vulgaris* dye extract. The absorption band at 3360 cm^{-1} is a consequence of the -OH stretching vibration, while the C=N bond stretching vibration is seen at 1632 cm^{-1} (Rotich *et al.*, 2022). The band found at around 1378 cm^{-1} was

linked to the extension stretching vibration of the C-H bond, whereas the absorption band peak at 1243 cm^{-1} was ascribed to the stretching vibration of the C-O bond of the carboxylic acid (Raouafi *et al.*, 2022). Located at 1054 cm^{-1} is a band connected to the symmetric stretching vibration of the C-O-C; centered at 945 is a band corresponding to the deformation of the C-H bond. The stretching vibrations of the C-COOH bond become visible at 832 cm^{-1}, all of these linked to betanin pigments (Batool *et al.*, 2024).

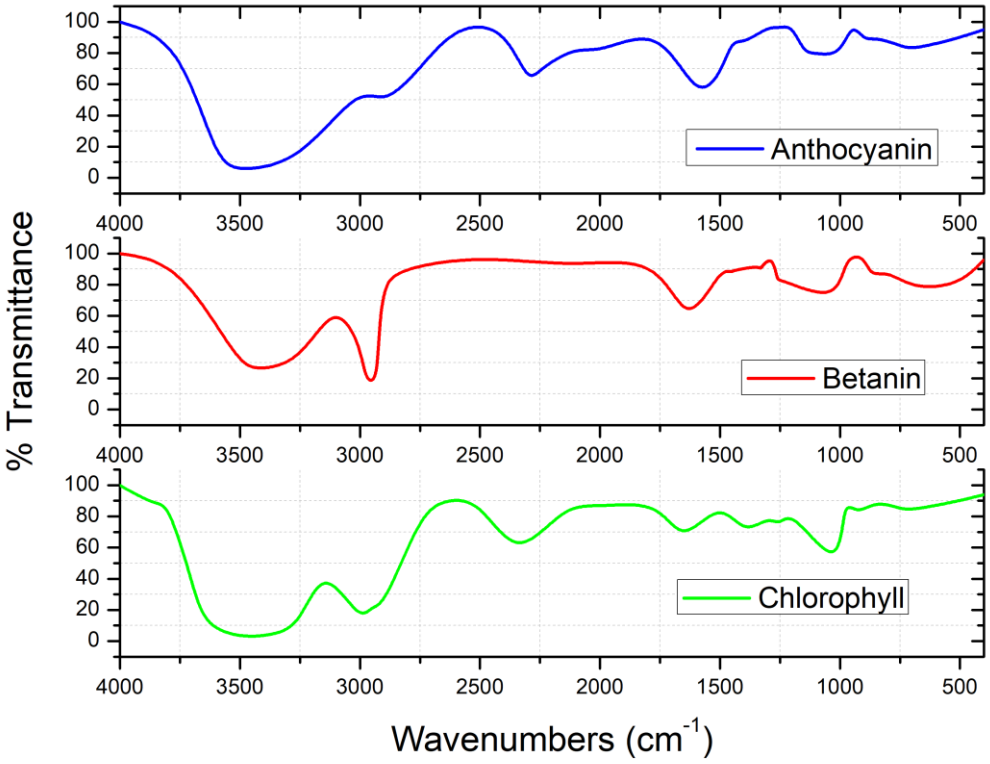

Figure 4.1: FTIR spectrum for dye extracts from (a) *Rubus fruticosus* (anthocyanin), (b) *Spinacia oleracea* (chlorophyll), and (c) *Beta vulgaris* (betanin)

4.2 Dye extracts optical absorbance

In DSSCs, dyes are used to sensitize TiO_2 semiconductors and are responsible for absorbing visible light to produce electricity (Omar *et al.*, 2020b). Two distinct classes of dyes exist: synthetic and natural (Dhorkule *et al.*, 2024). The utilization of plant-based natural dyes is attracting attention as they are easy to extract, eco-friendly, less expensive, and non-toxic.

The main light-harvesting pigments obtained from *Spinacia oleracea* leaves, *Rubus fruticosus* fruits, and *Beta vulgaris* roots are chlorophyll, anthocyanin, and betanin, respectively (Adeel *et al.*, 2019). Optical absorption spectra of these extracts were characterized using a Ultraviolet-visible (UV-Vis) spectrophotometer, to evaluate to what

extent the selected dyes absorb light and if there was any need for mixing them (Kharkwal & Dhawan, 2024). The absorption spectra of dyes obtained from *Spinacia oleracea* leaves, *Rubus fruticosus* fruits, and *Beta vulgaris* roots are displayed in Figure 4.2.

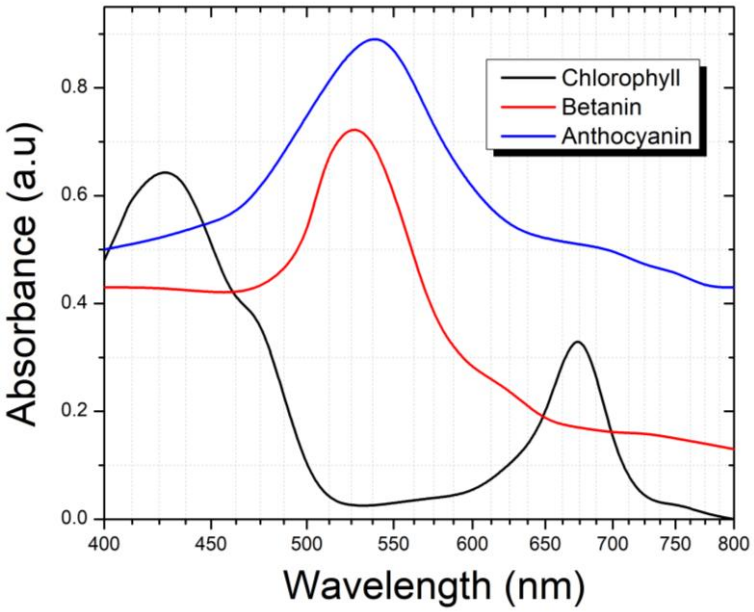

Figure 4.2: Absorbance spectra of mono dye extracts

Spinacia oleracea exhibits two major absorption peaks, one of which, observed in the spectral range of 380-500 nm (blue light), is broad, and another one is sharp at 660 nm (red light), which matches with the characteristic absorption peak of chlorophyll a pigments (Jaison *et al.*, 2023). The light between the peaks is not absorbed but reflected. This is the green light and the reason why leaves are green (Qiao *et al.*, 2025). Dyes extracted from *Rubus fruticosus* fruits reveal a wide absorption in the region of 450-650 nm (blue-green region), which is attributed to the presence of anthocyanins (Melo Miranda *et al.*, 2025). *Beta vulgaris* extract presents an absorption maximum at 525 nm (green region) that affirms the existence of betanin (Fauziah & Suryani, 2024). The visible range absorption of natural dyes fulfills the basic requirement for the use of a sensitizer in DSSC applications (Kokkonen *et al.*, 2021).

The absorption spectra of a combination of two dyes are depicted in Figure 4.3. Importantly, dye extract mixture from *Spinach oleracea* + *Beta vulgaris*, *Spinach oleracea* + *Rubus fruticosus,* and *Beta vulgaris* + *Rubus fruticosus*, all demonstrate strongly noticeable absorption peaks contained in the wavelength range of 400-800 nm.

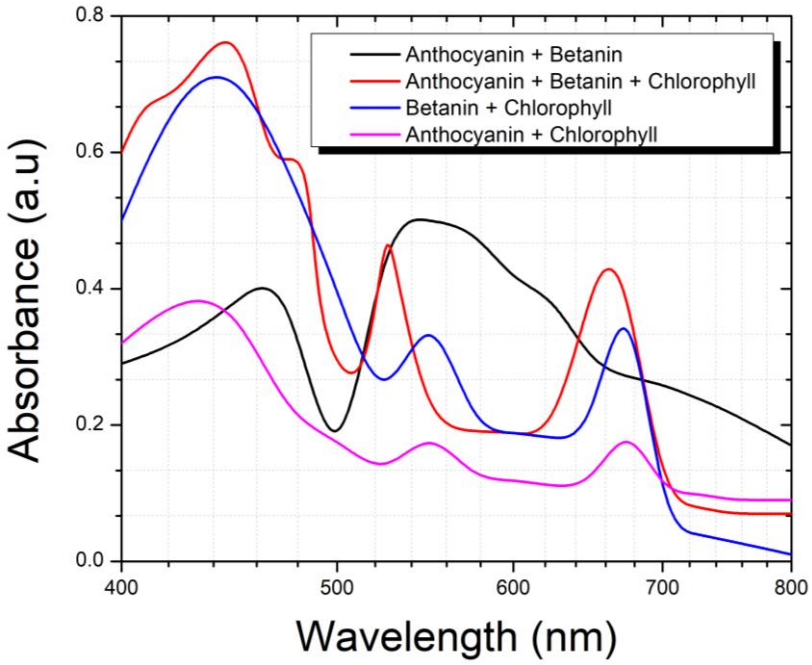

Figure 4.3: Absorbance spectra of dye mixture extracts

The spectrum for the combination *Spinach oleracia* + *Rubus fruticosus* has three peaks at 481 nm (effect of betanin dye), 548 nm, and 667 nm (effect of chlorophyll dye). The result for *Spinach oleracia* + *Beta vulgaris* dye mixture has three absorption peaks at wavelength 542, 560 nm (the contribution of betalain dye) and 682 nm (attributed to chlorophyll dye) and that for combination *Rubus fruticosus* + *Beta vulgaris* has three absorption peaks at wavelength 447 nm (the contribution of betalain dye), 550 nm (the contribution of anthocyanin dye) and 670 nm (effect of chlorophyll). While that of *Spinach oleracia* + *Rubus fruticosus* + *Beta vulgaris* exhibited three maxima at 453, 524, and 662 nm. These findings emphasize the fancy synergy of natural dyes and radiate their possibility for implementation in DSSCs. The corresponding values of quantified peak absorbance values are shown in Table 4.1.

Table 4.1: Quantified absorbance maxima and their peak absorbance values

Dye type	Wavelength peak (nm)	Absorbance (a.u)
chlorophyll	430, 660	0.32, 0.65
Anthocyanin	551	0.87
Betanin	525	0.71
Chlorophyll + Anthocyanin	481, 548, 667	0.18, 0.19, 0.37
Chlorophyll + Betanin	542, 560, 682	0.32, 0.35, 0.72
Anthocyanin + Betanin	447, 550, 670	0.28, 0.39, 0.51
Chlorophyll + Anthocyanin + Betanin	453, 524, 662	0.41, 0.45, 0.78

Meanwhile, the absorption characteristics of the three dye extracts combination comprising *Spinach oleracea* + *Rubus fruticosus* + *Beta vulgaris* exhibited two distinct peaks at 664 and 426-430 nm as depicted in Figure 4.3. The synergistic blending of all three natural dye extracts resulted in enhanced light-harvesting capabilities than single dye extracts, as witnessed by the higher absorbance values observed in the UV-Vis spectra.

These results signal the possibility of utilization of these mixtures in DSSCs, thereby highlighting the feasibility of employing natural dye blends in solar energy conversion technologies. Furthermore, each dye in the mixture showed stable absorption characteristics, signifying beneficial compatibility among these dyes, which is vital for the prolonged DSSC performance. The variation in the absorption characteristics resulting from the UV-Vis spectrophotometer is due to the varying nature of chromophores of dye extracts (Karuppaiah *et al*., 2023). Thus, compared to the individual extracts from *Spinacia oleracea*, *Rubus fruticosus,* and *Beta vulgaris*, the cocktail dyes can absorb a broader range of the solar spectrum, which in turn results in better photon-to-electric conversion efficiency in DSSC. The light absorption spectrum for the concocted dyes had peaks matching the contributions from single extracts (Kautsar *et al.*, 2021). The visible range of absorption of natural dyes fulfills the basic requirement for the use of a sensitizer in DSSC applications. Hence combination of natural dyes exhibits improved absorption in a wider range and can be used as an efficient light-harvesting application (Dhorkule *et al*., 2024; Onyemowo *et al.*, 2024).

4.3 The effect of co-sensitization of dyes on the photovoltaic performance of DSSC

Co-sensitization has emerged as an optimistic roadmap towards achieving panchromatic light harvesting and boost DSSC performance (Manz, 2022). In this research, the photovoltaic performance of DSSCs with chlorophyll, anthocyanin, and betanin dyes obtained from

Spinacia oleracea leaves *Rubus fruticosus* fruits, and *Beta vulgaris* roots, respectively, used as mono and co-sensitizers, were investigated. Current density-voltage curves (J-V curve) of the fabricated DSSCs were measured at standard test conditions using a solar simulator, generating 100 mW/cm^2 of irradiance (AM 1.5G) (Semenycheva *et al.*, 2021). The fill factor and PCE of the fabricated DSSCs were calculated using equations 2.7 and 2.9, respectively. The photovoltaic parameters of fabricated DSSCs are outlined in Table 4.2.

Table 4.2: Photovoltaic performance of chlorophyll, anthocyanin, and betanin dyes together with their mixture

Dye type	**Photovoltaic Parameters**			
	J_{SC} (mA/cm^2)	**V_{OC} (V)**	**Fill Factor (FF) (%)**	**Efficiency (PCE) (%)**
Chlorophyll	0.43	0.460	47.66	0.10
Anthocyanin	0.52	0.541	63.88	0.18
Betanin	0.81	0.582	81.69	0.39
Chlorophyll + Anthocyanin	0.49	0.511	53.48	0.13
Chlorophyll + Betanin	1.22	0.626	73.46	0.56
Anthocyanin + Betanin	0.74	0.594	67.64	0.30
Chlorophyll + Anthocyanin + Betanin	3.60	0.585	74.78	1.58

Among the mono-sensitized DSSCs, betanin-based DSSCs resulted in the best PCE of 0.39 % with a notably high V_{OC} of 0.58 V compared to other natural dyes presented in Table 4.1 and drawn in Figure 4.4 (Treat *et al.*, 2016).

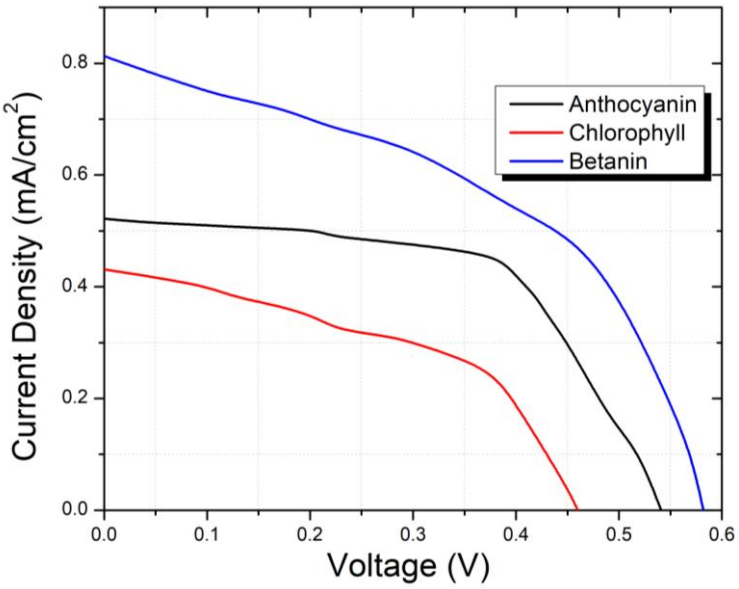

Figure 4.4: J-V curves for DSSCs sensitized with each single dye extract

An improvement in V_{oc} was due to the reduced charge recombination and improved carrier mobility (Yan *et al*., 2022). DSSCs employing anthocyanin dyes demonstrated a PCE of 0.18 % and a V_{oc} of 0.54 V. The superior performance was attributed to anthocyanin pigments found in *Rubus fruticosus*, as evidenced by the intense deep purple coloration (Ruba *et al.*, 2021). The chemical structure of anthocyanin is crucial to its ability to absorb sunlight and effectively transfer excitation energy to electrons in a DSSC's semiconductor layer (Abdulsalami *et al.*, 2023; Mejica *et al.*, 2022).

The DSSC utilizing chlorophyll-based dye extract displayed the least photovoltaic performance (Figure 4.4), with a PCE and J_{SC} of 0.09 % and 0.43 mA/cm^2, respectively. This diminished performance is attributed to the weak interaction between the chlorophyll dye molecules and TiO_2 semiconductors (Vallejo *et al*., 2025). The interfacial interaction between the TiO_2 semiconductor and the dye sensitizer is a critical determinant of the performance of DSSCs (Müller *et al.*, 2021). The notable high J_{SC} of 0.81 mA/cm^2 significantly (Vallejo *et al*., 2025) contributes to the superior performance of the DSSC based on betanin natural dye (Badawy *et al.*, 2022). Additionally, UV–Vis characterization of individual dye extracts shows that betanin and anthocyanin dye samples hold the broadest absorption spectra, directly agreeing with the photovoltaic performance of the DSSC device.

Conversely, the DSSCs employing cocktail dye extracts comprising chlorophyll + anthocyanin present heightened PCE in comparison to DSSCs based on individual samples of chlorophyll, as captured in Figure 4.5.

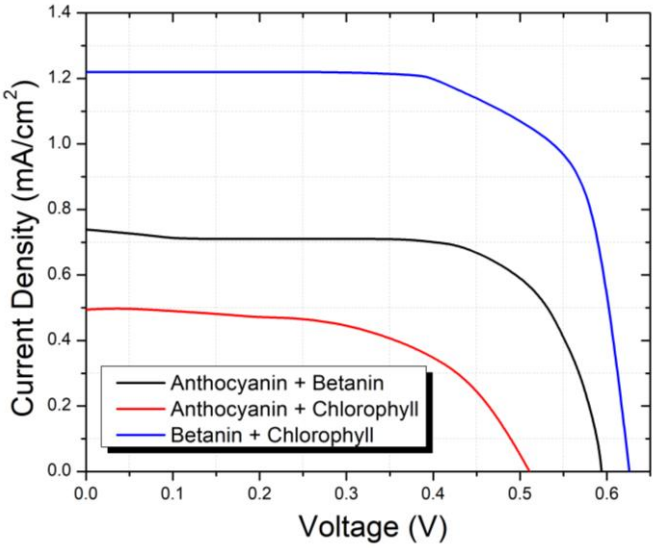

Figure 4.5: J-V curves for DSSC sensitized with a mixture of two dyes

Mixing dyes widens the optical absorption window and boosts the absorbance, resulting in increased DSSCs' photovoltaic performance (Rahman *et al*., 2023; Tamilselvan & Shanmugan, 2024; Xu *et al.*, 2022). DSSCs based on chlorophyll+ betanin indicates higher photovoltaic performance as opposed to DSSCs based on single chlorophyll and betanin dye extract (Figure 4.5). This improvement is attributed to the higher J_{SC} (1.22 mA/cm^2) observed in chlorophyll + betanin-sensitized DSSC contrasted with those utilizing single dyes. DSSCs employing a three-dye mixture of chlorophyll + anthocyanin + betanin achieved a notable PCE of 1.58 %, with FF, V_{OC}, and J_{SC} values of 74.78 %, 0.59 V, and 3.60 mA/cm^2, respectively.

The enhanced performance is mainly linked to the higher J_{SC} (3.6 mA/cm^2) observed in the cells relative to chlorophyll-based DSSCs (0.43 mA/cm^2), anthocyanin (0.52 mA/cm^2) and betanin (0.81 mA/cm^2). This refined performance could also be credited to the panchromatic light-capture, superior optical activity, and the appropriate energy levels (HOMO and LUMO) of the dye mixture. It can be seen that in Table 4.2 and Figure 4.6, FF is quite high compared to PCE.

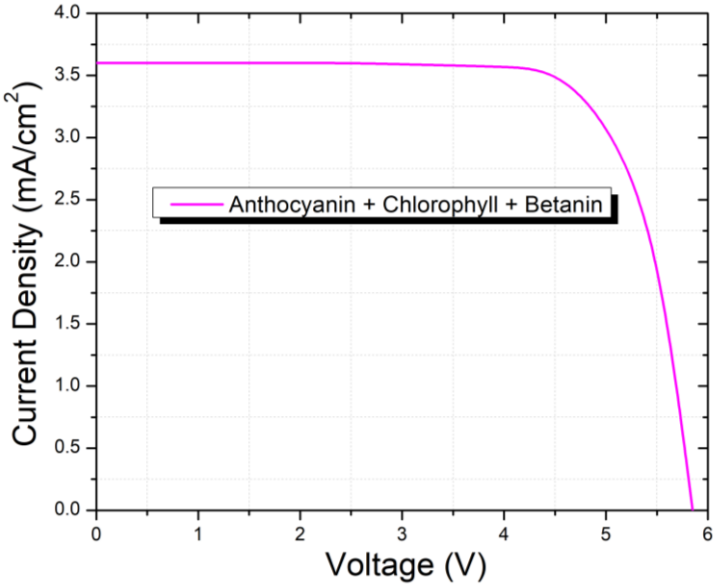

Figure 4.6: J-V curves for DSSCs sensitized with a mixture of three dyes

This is a common phenomenon as PCE does not only depend on maximum power output but also on J_{SC} and V_{OC}. A large fill factor (FF) implies that there are good charge transport and low internal losses of a solar cell, but not a high PCE. PCE relies on three major parameters, that is, Voc, J_{SC}, and FF. Thus, low V_{OC} or low J_{SC} caused by low light absorption efficiencies will cause low overall PCE index even in cases with high FF. In this way the cell can have a high internal charge collection efficiency (high FF), however it can contribute very low total power output because of low photocurrent (Lin *et al.*, 2023).

Co-sensitization of natural dye-based DSSCs shows an improved PCE as a result of broader absorption in the visible region (Kharkwal *et al.*, 2021). In addition, hybrid dye-sensitization may suppress the recombination of charge carriers and increase electron injection lifetime owing to the time delay in electron injection by the intermediate excited level of adjacent dye molecules (Zeng *et al.*, 2021). However, a reduced J_{SC} value of mono-sensitized DSSCs in Table 4.2 is attributed to a slim absorption spectrum of natural dyes.

Natural dyes have shown overall PCEs below 1 %, arising from weak interaction between dye extracts and TiO_2 semiconductors. However, extending the absorption wavelength range through the combination of different dye extracts enhances the ability to capture a broader spectrum (panchromatic shift) of visible light, thereby improving the overall PCE of DSSCs.

The cocktail dye extracts containing chlorophyll and anthocyanin signify a remarkable absorption range as opposed to individual dye solutions.

4.4 The effect of annealing temperature of photo anodes on the photovoltaic performance of DSSC

In this study, different annealing temperatures were applied to TiO_2 films to ascertain their effects on DSSC overall power conversion efficiency (PCE). Before annealing, the TiO_2 is usually amorphous with loosely arranged nanoparticles, but after annealing it induces crystallinity. The logic behind annealing before dye loading at different temperatures is to remove moisture, decompose ethyl cellulose and to obtain crystalline TiO_2 photoanodes. These films were annealed at temperatures varying from 250 °C to 550 °C (steps of 100 °C) and used to fabricate DSSCs whose photovoltaic characteristics were later evaluated. Before photovoltaic testing, electrodes alignment was checked to eliminate short-circuit between the photoanode and counter electrode, then connected to a solar simulator for J-V measurements. To avoid dye degradation, allow the annealed TiO_2 to cool down slowly then immerse the film into dyes sensitizer at room temperature (25 °C). A dye mixture of all three dyes (chlorophyll, anthocyanin, and betanin) was chosen as a sensitizer because it yielded higher photovoltaic performance than individual dye DSSCs in the previous tests. Figure 4.7 present the J–V characteristics curves for the assembled DSSCs with TiO_2 films annealed at varying temperatures, while a summary of the photovoltaic properties of these DSSCs is compiled in Table 4.3. From this table, photovoltaic properties were found to be reliant on the annealing temperature of TiO_2 films.

The PCE measurements from annealed films were optimal when the temperature reached 450 °C. Table 4.3 demonstrates that the low temperature (250 °C) annealed films present lower PCEs because they generate reduced short-circuit current density (J_{SC}). The TiO_2 films exposed to 250 °C temperature maintain impurities and structural imperfections due to the remaining organic compounds found in paste products (Lukong *et al*., 2022; Pant *et al.*, 2019). These defects create constraints for dye-loading as they limit the accessible surface area available on the material. Annealing TiO_2 film at lower temperatures leads to a film that has poor crystalline, defective and leads to weak adhesion of dyes. This in turn results in low J_{SC}, low V_{OC} and poor PCE. Too high annealing temperatures lead to grain growth and FTO substrate damage hence result in moderate J_{SC}, low V_{OC} and reduced PCE. On the other hand, optimal temperatures (450 °C) results in a film that is highly crystalline with good interparticle contact leading to high PCE.

Table 4.3: Photovoltaic performance of DSSCs sensitized in chlorophyll + anthocyanin + betanin dye mixture for a duration of 40 h with photo anodes annealed at varying temperatures

Temperatures (°C)	**Photovoltaic parameters**			
	J_{SC} (mA/cm^2)	V_{OC} (V)	Fill Factor (FF) (%)	Efficiency (PCE) (%)
250	1.8	0.50	68.83	0.62
350	2.1	0.55	64.52	0.75
450	3.6	0.59	74.78	1.58
550	3.4	0.56	70.30	1.34

The open circuit potential (V_{OC}) and J_{SC} production of these devices gradually improved as the annealing temperatures rose from 250 °C to 450 °C. The light-harvesting capability of dye molecules grows stronger because the thermal decomposition process expands the surface area of TiO_2 films where dye adsorption occurs (Joseph *et al*., 2020; Liu *et al.*, 2024; Manikandan *et al.*, 2025). Optimal annealed TiO_2 films led to high crystallinity and good interparticle bonds enhancing J_{SC} up to 3.6 mA/cm² at 450 °C. this is made possible by having a film that has strong dye adsorption leading to efficient electron injection. The J_{SC} value decreased to 3.4 mA/cm² as the PCE declined to 1.34 % when the annealing temperature reached 550 °C.

The V_{OC} at 350 °C was 0.55 V, then elevated to 0.59 V at 450 °C before declining to 0.56 V at 550 °C. When using lower annealing temperatures, the electrons moving from the dye to the TiO_2 conduction band will tend to recombine at defective locations. The recombination process lowers conduction band electron density, which results in decreased V_{OC} values. The conversion efficiency of TiO_2 annealed at 450 °C exceeds that of TiO_2 annealed at 250 °C because of its better anchoring properties to the dye molecules (Kashif *et al.*, 2020). Therefore, the performance of TiO_2 films annealed at 450 °C is deemed superior in comparison to the performances of TiO_2 films annealed at 250 °C, 350 °C and 550 °C. Increased crystallinity, enlarged grain size, and improved transparency of conducting glass with surfactant-free pores enhance the photovoltaic performance of the fabricated cell. To achieve both maximum dye loading capability and efficient electron transport, the application of moderate heat at 450°C becomes essential since it sustains TiO_2 nanoparticles' large specific surface area (Nagaraj *et al.*, 2025). The performance of the natural dyes measured in this research matches what researchers have published previously.

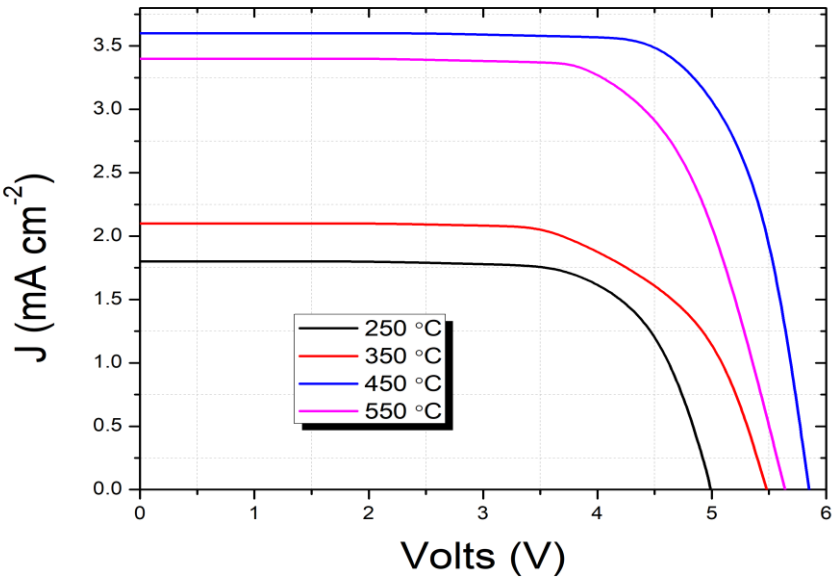

Figure 4.7: J-V curves for DSSCs sensitized in chlorophyll + anthocyanin + betanin dye mixture for a duration of 40 h with photo anodes annealed at varying temperatures

4.5 The effect of soaking duration on the photovoltaic performance of DSSC

A cocktail of three dyes (chlorophyll, anthocyanin, and betanin) was selected for further study as it showed better photovoltaic performance in comparison to individual extracts. After annealing TiO_2 film and cooling down to room temperature, sensitization took place in the optimal dye mixture at different temperatures from 20 h to 50 h and then used to fabricate DSSCs. A solar simulator was used to determine the fabricated DSSCs performance from which the performance of the cells was evaluated. The soaking process was carried out away from light for maximum dye adsorption onto the TiO_2 film.

Table 4.4 and Figure 4.8 compare the performance of DSSCs with TiO_2 films sensitized in chlorophyll + anthocyanin + betanin dye mixture at different soaking durations of 20, 30, 40, and 50 hours.

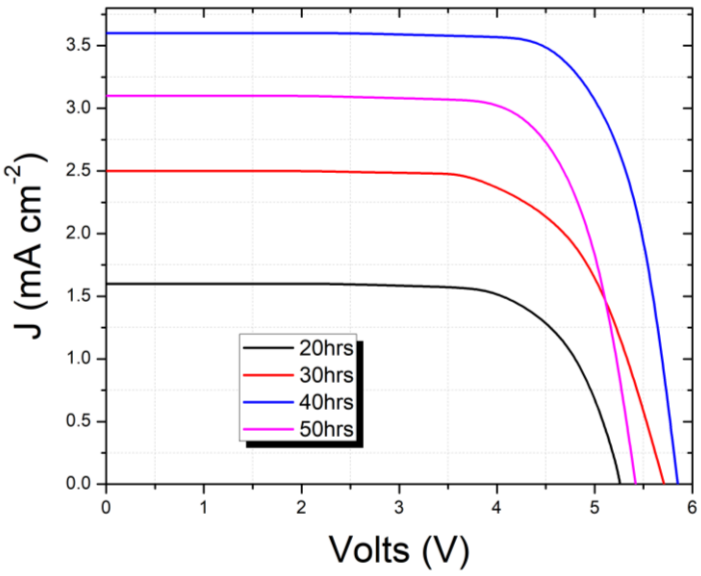

Figure 4.8: J-V curves for DSSCs annealed at 450 °C and sensitized in chlorophyll + anthocyanin + betanin dye mixture (1:1:1 volume ratio) at different dye-loading times

It is recorded that open-circuit voltage (V_{OC}) and short-circuit current density (J_{SC}) progressively increase with the increase in soaking time up to 40 h and decrease suddenly when the soaking duration is increased to 50 h, as shown in Table 4.4. The V_{OC} and J_{SC} become more pronounced at 40h dye-adsorption time. The decrease in J_{SC} and V_{OC} at 50 h soaking time can be linked to recombination in the TiO_2 film. The fill factor (FF) is less for shorter dye adsorption times (20 h) but shows higher values at longer dye adsorption times (40 h). Higher values of FF produce more efficient cells.

Table 4.4: Photovoltaic performance DSSCs annealed at 450 °C and sensitized in chlorophyll + anthocyanin + betanin dye mixture (1:1:1 volume ratio) at different dye-loading times

Dye-loading time (hours)	**Photovoltaic parameters**			
	J_{SC} (mA/cm^2)	V_{OC} (V)	Fill Factor (FF) (%)	Efficiency (PCE) (%)
20	1.6	0.53	73.46	0.56
30	2.5	0.57	72.54	0.64
40	3.6	0.59	74.78	1.58
50	3.1	0.54	74.12	1.44

The power conversion efficiency (PCE) was less than 20 h dye-adsorption time and then started increasing up to 40 h. The PCE of DSSC increased from 0.56 % to 1.58 % for 20 h to 40 h of sensitization time and decreased after increasing soaking time to 50 h (1.44 %). The PCE improvement was caused by enhanced dye layer coverage, which optimized the charge transfer between the TiO_2 conduction band and electrolyte. The photo anodes transferred a greater number of electrons because of better charge transfer capabilities. The overall PCE received additional electrons, which were distributed through the external circuit because of these changes.

The device developed abnormal behavior following the expiration of the optimal immersion time (40 h). The photovoltaic performance of the system started to diminish after reaching this phase. The continuous exposure to dye sensitizer resulted in performance degradation of DSSC because the sensitizer became less stable during extended soaking periods (Chalkias *et al.*, 2020). Higher soaking duration causes a decrease in V_{OC} and J_{SC} because the multilayer formation results in increased recombination effects. It is acknowledged that the increase in dye-loading time (50 h) led to dye aggregation that triggers the quenching of photo-excited electrons and consequently leads to the decline in charge injections (Magiswaran *et al.*, 2022).

The results of this study show that the DSSCs with 40 h sensitization time displayed complete dye adsorption within the DSSC photoanodes. However, dye impregnations are limited by dye concentration. It is observed that PCE increases as the dye-soaking time increases. This outcome suggested that longer dye-loading contributed to enhanced DSSC performance (Jagtap *et al*., 2021). The degradation and loss of activity of dye molecules occurred due to their instability when subjected to extended immersion durations of up to 50 h. Natural dyes are considered be unstable and can degrade under prolonged exposure to light, heat, and oxygen (Alegbe & Uthman, 2024 ; Pizzicato *et al*., 2023). This outcome can lead to a decrease in the photovoltaic response of the DSSCs. Therefore, to acquire the best PCE, the dye sensitization time on TiO_2 photo anodes must be controlled. Accordingly, the outcome of this investigation recommended that a dye-loading time of 40 h was a better starting point for attaining optimal performance.

CHAPTER FIVE
SUMMARY, CONCLUSIONS, AND RECOMMENDATIONS

5.1 Summary

This research prioritized extraction, characterization, and co-sensitization of chlorophyll, anthocyanin, and betanin natural dyes for application in dye-sensitized solar cells (DSSCs), highlighting how dye extract properties and semiconductor layer processing parameters impact device photovoltaic performance. Chlorophyll, anthocyanin, and betanin, were obtained from fresh *Spinacea oleracea* leaves, *Rubus fruticosus* fruits, and *Beta vulgaris* roots, respectively. Plant materials were first cleaned thoroughly using distilled water to remove dirt and then cut into small pieces. A 100 g portion of the sliced plant material were placed in a blender and blended for 2.0 minutes. Chlorophyll was extracted using 80 % ethanol, anthocyanin with methanol and acidified HCl and betanin was extracted using 0.1 % ethanol HCl V/V ethanol. The mixtures were stirred for 40 minutes then filtered using a Whatman filter paper. The filtrates were mixed with acidified (hydrochloric acid) methanol to remove unwanted proteins. The dye solutions purple (anthocyanin), green (chlorophyll), and deep red (betanin) were kept in an amber bottle and then stored in a refrigerator at 4 ℃. Cocktail dyes were formulated by mixing single dyes in 1:1 (two different dyes) and 1:1:1 (three different dyes) volume ratio to examine their effect on the absorption spectra.

Fourier Transform Infrared (FTIR) spectroscopy was used to analyze functional groups present in dye extracts within the wave number 4000–400 cm^{-1}. Anthocyanin spectra presented intense peaks at 3332 cm^{-1} (–OH stretching), 3016 cm^{-1} (C-H stretching), 1778 cm^{-1} (C=O stretching), and 1608 cm^{-1} (C=C stretching). Chlorophyll showed peaks at 1692 cm^{-1} (C=O stretching), 3558 cm^{-1} (–OH stretching), and 1064 cm^{-1} (C–O bonds), while betanin displayed 1632 cm^{-1} (C=N) and 3360 cm^{-1} (–OH). These results indicate the presence of functional groups in anthocyanin, chlorophyll, and betanin dyes essential for anchorage onto TiO_2 semiconductor, visible light absorption and charge transfer for efficient DSSCs fabrication.

Optical absorbance characteristics of single and mixture dye extracts were analyzed using ultraviolet-visible (UV-Vis) spectroscopy within the 400–800 nm wavelength range. *Spinacea Oleracea* dye exhibited two major absorption peaks at the wavelength range of 380-500 nm (blue light), and another sharp peak at 660 nm (red light), showing the presence of chlorophyll. Chlorophyll+ anthocyanin had three absorption peaks at wavelengths 481 nm, 548 nm, and 667 nm. The result for Chlorophyll+ betanin dye had three absorption peaks at wavelength 542 nm, 560, and 682 nm and that for combination anthocyanin+ betanin had three absorption peaks at

wavelength 447 nm, 550 nm, and 670 nm. The absorption characteristics of the ternary dye mixture (chlorophyll + anthocyanin + betanin) exhibited three distinct peaks at 453, 524 and, 662 nm. Concocted dyes exhibited panchromatic shift, signifying enhanced light capture.

Doctor-blading method was used to coat FTO with TiO_2 thin films on FTO. These films were annealed at different temperatures varying from 250 to 550 °C 9in steps of 100 °C to examine the impact of annealing temperature on photovoltaic performance of fabricated DSSCs. Current density-voltage (J-V) curves indicated that TiO_2 thin films annealed at 450°C produced cells with optimal photovoltaic performance of J_{SC} (3.6 mA/cm^{-2}), V_{OC} (0.59V) and PCE (1.58). Too high annealing temperatures (550°C) lead to grain growth and FTO substrate damage hence resulted in moderate J_{SC}, low V_{OC} and reduced PCE of 3.4 mA/cm^{-2},0.56 V and 1.34 % respectively. Low temperature (250 °C) annealed films presented lower PCEs of 0.62 % with lower J_{SC} of 1.8 mA/cm^{-2} owing to the fact that these cells maintain impurities and structural imperfections after annealing.

Dye-sensitization duration experiments were carried out by immersing annealed TiO_2 films in individual and blended dye solutions for 20, 30, 40, and 50 hours at room temperature. It was noted that V_{OC} and J_{SC} gradually increased with the increase in soaking time up to 40 h (3.6 mV/cm^{-2} and 0.59V)) and decreased suddenly when the soaking duration was increased to 50 h (3.1 mV/cm^{-2} and 0.54V). The decrease in J_{SC} and V_{OC} at 50 h soaking time can be attributed formation of multilayer adsorption which leads to energy injection losses and ultimately recombination in the TiO_2 film.

In summary, this study established that natural dyes can be successfully extracted and characterized for application in DSSCs, with FTIR spectroscopy validating significant functional groups for TiO_2 anchorage, light absorption, and charge transfer. UV-Vis spectroscopy emphasized the benefits of co-sensitizing dyes in achieving panchromatic light absorption. Semiconductor film annealing temperature and dye-sensitization time were key variables affecting photovoltaic performance of DSSCs, with optimized annealing and dye-loading time yielding the highest PCE. Concocted dyes, particularly chlorophyl+ anthocyanin +betanin mixture, demonstrated synergistic influence on J_{SC} and V_{OC} and overall DSSC PCE, promoting the prospect of natural dye-based DSSC as eco-friendly substitute to ruthenium-based dyes. These results present a framework for future study on optimizing the stability and efficiency of sustainable, nature-inspired DSSC devices.

From the results of this study, future research can be done on DSSCs by varying the characteristics of the photoanodes. This can be done by purifying and mixing dyes before the

adsorption process, annealing the TiO_2 films at optimal temperature of 450 °C, and optimizing dye loading time to 400- 450 °C.

5.2 Conclusions

i. Chlorophyll, anthocyanin, and betanin dyes were successfully extracted from *Spinacea oleracea* leaves, *Rubus fruticosus* fruits, and *Beta vulgaris* roots, respectively, and contained anchoring sites ideal for TiO_2 attachment.
ii. Mixed dye extracts displayed wider absorption solar spectrum as compared to individual extracts, optimizing photon capture, dye excitation and charge transfer in DSSC.
iii. DSSC sensitized with TiO_2 films annealed at 450 °C attained optimal photovoltaic parameters.
iv. DSSC sensitized with TiO_2 films with dye-loading time of 40 hours achieved optimal power conversion efficiency.

5.3 Recommendations

i. Purification of dye extracts can be explored after extraction to improve concentration and enhance efficiency of fabricated DSSCs.
ii. Co-sensitization of natural dyes with ruthenium-based dyes can be investigated with the aim of widening absorption window and improving stability.
iii. Keep TiO_2 film annealing temperature at 450 °C- 500 °C for optimal dye adsorption and efficient charge transport.
iv. Examine the effects of dye DSSC photovoltaic performance on annealing TiO_2 film after dye loading.

REFERENCES

Abdellah, I. M. (2025). Molecular engineering and electrolyte optimization strategies for enhanced performance of Ru (ii) polypyridyl-sensitized DSSCs. *RSC advances*, *15*(13), 9763-9786. https://doi.org/10.1039/D5RA01470K

Abdulsalami, I. O., Semire, B., & Bello, I. A. (2023). Theoretical examination of efficiency of anthocyanidins as sensitizers in dye-sensitized solar cells. *Physical Sciences Reviews*, *8*(1), 33-50. https://doi.org/10.1515/psr-2019-0133

Adak, S., & Cangi, H. (2024). Development software program for finding photovoltaic cell open-circuit voltage and fill factor based on the photovoltaic cell one-diode equivalent circuit model. *Electrical Engineering*, *106*(2), 1251-1264. https://doi.org/10.1007/s00202-023-02082-0

Adeel, S., Rehman, F.-U., Rafi, S., Zia, K. M., & Zuber, M. (2019). Environmentally friendly plant-based natural dyes: extraction methodology and applications. *Plant and Human Health Aspects*, *2*(3), 383-415. https://doi.org/10.1007/978-3-030-03344-6_17

Aghazada, S., & Nazeeruddin, M. K. (2018). Ruthenium complexes as sensitizers in dye-sensitized solar cells. *Inorganics*, *6*(2), 1-34. https://doi.org/10.3390/inorganics6020052

Agrawal, A., Siddiqui, S. A., Soni, A., & Sharma, G. D. (2022). Advancements, frontiers and analysis of metal oxide semiconductor, dye, electrolyte and counter electrode of dye sensitized solar cell. *Solar Energy*, *233*(2), 378-407. https://doi.org/10.1016/j.solener.2022.01.027

Ahliouati, M., El Otmani, R., Kandoussi, K., & Boutaous, M. H. (2025). Dynamic thermal analysis comparing the energy efficiency of a photovoltaic module under varying meteorological conditions at two distinct Moroccan sites. *Theoretical and Applied Climatology*, *156*(5), 1-18. https://doi.org/10.1007/s00704-025-05488-x

Al-horaibi, S. A., Al-Odayni, A.-B., Alezzy, A., ALSaeedy, M., Al-Adhreai, A., Saeed, W. S., & Hasan, A. (2023). Novel Squaraine dyes for high-performance in dye-sensitized solar cells: Photophysical properties and adsorption behavior on TiO2 with different anchoring groups. *Journal of Molecular Structure*, *1290*(3), 1-15. https://doi.org/10.1016/j.molstruc.2023.135943

Al-Rikabi, I. J., Omara, A. A., Abuelnour, M. A., Abuelnuor, A. A., Mohamed, A. E., & Ismail, N. A. (2025). Renewable Energy in Sudan: Current Status and Future Prospects. *Engineering Reports*, *7*(1), 1-30. https://doi.org/10.1002/eng2.13116

Alegbe, E. O., & Uthman, T. O. (2024). A review of history, properties, classification, applications and challenges of natural and synthetic dyes. *Heliyon*, *10*(13), 1-19. https://doi.org/10.1016/j.heliyon.2024.e33646

Alhaji Abubakar, A., Sadiq Abubakar, Y., Mohammed Kimpa, I., Ibrahim Olalonpe, S., & Isah Uthman, K. (2025). Exploring the Impact of Surface Treatments on Electron Transport and Recombination in DSSC Plasmonic Photoanodes: A Systematic Review. *Plasmonics*,*7*(1), 1-25. https://doi.org/10.1007/s11468-025-03011-6

Alim, M. A., Repon, M. R., Islam, T., Mishfa, K. F., Jalil, M. A., Aljabri, M. D., & Rahman, M. M. (2022). Mapping the Progress in natural dye-sensitized solar cells: materials, parameters and durability. *ChemistrySelect*, *7*(23), 1-23. https://doi.org/10.1002/slct.202201557

AM Al-Alwani, M., Al-Mashaan, A. B. S., & Abdullah, M. F. (2019). Performance of the dye-sensitized solar cells fabricated using natural dyes from Ixora coccinea flowers and Cymbopogon schoenanthus leaves as sensitizers. *International Journal of Energy Research*, *43*(13), 7229-7239. https://doi.org/10.1002/er.4747

Ambedkar, B. B., & Pradesh, U. (2019). Betalian pigments extracted from the red beet and its potential uses as natural dyes in new food product development. *J. Pharmacogn. Phytochem*, *8*(6), 991-993.

Amogne, N. Y., Ayele, D. W., & Tsigie, Y. A. (2020). Recent advances in anthocyanin dyes extracted from plants for dye sensitized solar cell. *Materials for Renewable and Sustainable Energy*, *9*(4), 1-16. https://doi.org/10.1007/s40243-020-00183-5

Andualem, A., & Demiss, S. (2018). Review on dye-sensitized solar cells (DSSCs). *Edelweiss Appli Sci Tech*, *2*(2), 145-150. https://doi.org/10.33805/2639-6734.103

Ansir, R., Ullah, N., Ünlü, B., Shah, S. M., & Özacar, M. (2021). Effect of annealing temperatures on performance of DSSCs fabricated using Ag or Pd@ C@ ZnO composites as photoanode materials. *Solar Energy*, *224*(1), 617-628. https://doi.org/10.1016/j.solener.2021.06.042

Arka, G. N., Prasad, S. B., & Singh, S. (2021). Comprehensive study on dye sensitized solar cell in subsystem level to excel performance potential: A review. *Solar Energy*, *226*(1), 192-213. https://doi.org/10.1016/j.solener.2021.08.037

Arunkumar, A., & Anbarasan, P. (2023). Computational study on D-π-A-based electron donating and withdrawing effect of metal-free organic dye sensitizers for efficient dye-sensitized solar cells. *Journal of Computational Biophysics and Chemistry*, *22*(8), 1115-1124. https://doi.org/10.1142/S2737416523420139

Aslam, A., Mehmood, U., Arshad, M. H., Ishfaq, A., Zaheer, J., Khan, A. U. H., & Sufyan, M. (2020). Dye-sensitized solar cells (DSSCs) as a potential photovoltaic technology for the self-powered internet of things (IoTs) applications. *Solar Energy*, *207*(2), 874-892. https://doi.org/10.1016/j.solener.2020.07.029

Awad, Z. A., Eida, M. A., Soliman, H. S., Alkaramani, M. A., Elbadwy, I. G., & Hassabo, A. G. (2025). The psychological effect of choosing colors in advertisements on stimulating human interaction. *Journal of Textiles, Coloration and Polymer Science*, *22*(1), 289-298. https://doi.org/10.21608/jtcps.2024.259790.1323

Awsha, A., Alazoumi, S., & Elhub, B. (2021). A Review on the development of TiO2 photoanode for Solar Applications. *Albahit J Appl Sci*, *2*(2), 9-16.

Azlina, A., Mamat, M., Che Soh, Z., Rahman, M., Othman, N., Marina, M.,…Abdullah, M. (2023). Mitragyna speciosa dye sensitiser as the light-harvesting molecules for dye-sensitised solar cells. *Jurnal Teknologi (Sciences & Engineering)*, *85*(1), 107-113. https://doi.org/10.11113/jurnalteknologi.v85.18695

Baby, R., Nixon, P. D., Kumar, N. M., Subathra, M., & Ananthi, N. (2022). A comprehensive review of dye-sensitized solar cell optimal fabrication conditions, natural dye selection, and application-based future perspectives. *Environmental Science and Pollution Research*, *29*(1), 371-404. https://doi.org/10.1007/s11356-021-16976-8

Badawy, S. A., Abdel-Latif, E., Fadda, A. A., & Elmorsy, M. R. (2022). Synthesis of innovative triphenylamine-functionalized organic photosensitizers outperformed the benchmark dye N719 for high-efficiency dye-sensitized solar cells. *Scientific Reports*, *12*(1), 1-17. https://doi.org/10.1038/s41598-022-17041-1

Bandara, T., Gunathilake, S., Dissanayake, M., Pemasiri, B., Albinsson, I., & Mellander, B.-e. (2024). A review of the development of graphene-incorporated dye-sensitized solar cells. *Ionics*, *30*(11), 6789-6809. https://doi.org/10.1007/s11581-024-05752-6

Barichello, J., Mariani, P., Vesce, L., Spadaro, D., Citro, I., Matteocci, F.,…Calogero, G. (2024). Bifacial dye-sensitized solar cells for indoor and outdoor renewable energy-based application. *Journal of Materials Chemistry C*, *12*(7), 2317-2349. https://doi.org/10.1039/D3TC03220E

Basu, P. (2024). Brief history of semiconductor science and technology and India's role in the decade after the invention of transistor. *Indian Journal of History of Science*, *59*(2), 204-215. https://doi.org/10.1007/s43539-024-00125-4

Batool, F., Iqbal, N., Adeel, S., Azeem, M., Hussaan, M., & Mia, R. (2024). Sugar beet (Beta vulgaris L.) leaves as natural colorant for cotton dyeing using an ecofriendly approach

toward industrial progress. *Science Progress*, *107*(3), 1-22. https://doi.org/10.1177/00368504241271737

Belmahdi, B. (2025). Comparative study of parameter extractions of photovoltaic modules using analytical and numerical approaches. *Frontiers in Energy Research*, *13*(1), 1-15. https://doi.org/10.3389/fenrg.2025.1501335

Bera, M. K., Pal, P., & Malik, S. (2020). Solid-state emissive organic chromophores: design, strategy and building blocks. *Journal of Materials Chemistry C*, *8*(3), 788-802. https://doi.org/10.1039/C9TC04239C

Bernardi, T., Bortolini, O., Massi, A., Sacchetti, G., Tacchini, M., & De Risi, C. (2019). Exploring the synergy between HPTLC and HPLC-DAD for the investigation of wine-making by-products. *Molecules*, *24*(19), 1-16. https://doi.org/10.3390/molecules24193416

Bist, A., & Chatterjee, S. (2021). Review on efficiency enhancement using natural extract mediated dye-sensitized solar cell for sustainable photovoltaics. *Energy Technology*, *9*(8), 1-19. https://doi.org/10.1002/ente.202001058

Blanco, E., Domínguez, M., González-Leal, J., Márquez, E., Outón, J., & Ramírez-del-Solar, M. (2018). Insights into the annealing process of sol-gel TiO2 films leading to anatase development: The interrelationship between microstructure and optical properties. *Applied Surface Science*, *439*(3), 736-748. https://doi.org/10.1016/j.apsusc.2018.01.058

Błaszczyk, A. (2018). Strategies to improve the performance of metal-free dye-sensitized solar cells. *Dyes and pigments*, *149*(2), 707-718. https://doi.org/10.1016/j.dyepig.2017.11.045

Boro, B., Gogoi, B., Rajbongshi, B., & Ramchiary, A. (2018). Nano-structured TiO2/ZnO nanocomposite for dye-sensitized solar cells application: A review. *Renewable and Sustainable Energy Reviews*, *81*(2), 2264-2270. https://doi.org/10.1016/j.rser.2017.06.035

Bulavko, G. (2024). Organic photovoltaics: A journey through time, advancements, and future opportunities. *History of science and technology*, *14*(1), 10-32.

Cachorro, V. E., Antuña-Sanchez, J. C., & de Frutos, Á. M. (2021). SSolar-GOA v1. 0: a simple, fast, and accurate Spectral SOLAR radiative transfer model for clear skies. *Geoscientific Model Development Discussions*, *2021*, 1-42. https://doi.org/10.5194/gmd-15-1689-2022

Chalkias, D., Loizos, D., & Papanicolaou, G. (2020). Evaluation and prediction of dye-sensitized solar cells stability under different accelerated ageing conditions. *Solar Energy*, *207*(3), 841-850. https://doi.org/10.1016/j.solener.2020.06.115

Chang, H., & Lo, Y.-J. (2010). Pomegranate leaves and mulberry fruit as natural sensitizers for dye-sensitized solar cells. *Solar Energy*, *84*(10), 1833-1837. https://doi.org/10.1016/j.solener.2010.07.009

Chaudhari, A., Kumar, A., Kumar, S., & Kushwaha, S. (2024). Synthesis of TiO2 nanoparticles by green approach: Application as photoanode for dye-sensitized solar cells. *Materials Research Bulletin*, *179*(2), 1-11. https://doi.org/10.1016/j.materresbull.2024.112909

Chavan, G. T., Kim, Y., Khokhar, M. Q., Hussain, S. Q., Cho, E.-C., Yi, J.,…Jeon, C.-W. (2023). A brief review of transparent conducting oxides (TCO): the influence of different deposition techniques on the efficiency of solar cells. *Nanomaterials*, *13*(7), 1-19. https://doi.org/10.3390/nano13071226

Chen, D., Tong, Z., Rao, Q., Liu, X., Meng, H., & Huang, W. (2024). High-performance black copolymers enabling full spectrum control in electrochromic devices. *Nature communications*, *15*(1), 1-9. https://doi.org/10.1038/s41467-024-52430-2

Chen, J., Vishart, A. L., Sauer, S. P., & Mikkelsen, K. V. (2023). Theoretical Investigations of Dye-Sensitized Solar Cells. *Journal of Nanotechnology and Nanomaterials*, *4*(2), 38-54. https://doi.org/10.33696/Nanotechnol.4.042

Chen, Z., Li, F., & Huang, C. (2007). Organic D-π-A dyes for dye-sensitized solar cell. *Current Organic Chemistry*, *11*(14), 1241-1258. https://doi.org/10.2174/138527207781696008

Chen, Z., Yang, Y., Lou, H., & Wang, H. (2025). Effect of Heat Treatment on the Grain Boundary Character Distribution and Bending Properties of Fine-Grained Phosphorus Bronze. *Materials*, *18*(9), 1-19. https://doi.org/10.3390/ma18091941

Coppola, C., Parisi, M. L., & Sinicropi, A. (2023). The role of organic compounds in dye-sensitized and perovskite solar cells. *Energies*, *16*(2), 1-4. https://doi.org/10.3390/en16020573

Danfá, S., Martins, R. C., Quina, M. J., & Gomes, J. (2021). Supported TiO2 in ceramic materials for the photocatalytic degradation of contaminants of emerging concern in liquid effluents: a review. *Molecules*, *26*(17), 1-20. https://doi.org/10.3390/molecules26175363

Das, U., Das, A., Islam, M., Das, R., & Das, A. K. (2024). Chemistry Behind the Mystery of Colors of Different Objects–Part 1. *Resonance*, *29*(12), 1643-1668. https://doi.org/10.1007/s12045-024-1643-7

Dey, T. (2021). Role of earth-abundant selenium in different types of solar cells. *Journal of Electrical Engineering*, *72*(2), 132-139. https://doi.org/10.2478/jee-2021-0019

Dhafina, W. A., Salleh, H., Daud, M. Z., & Ghazali, M. S. M. (2018). Low cost dye-sensitized solar cells based on zinc oxide and natural anthocyanin dye from Ardisia elliptica fruits. *Optik*, *172*(1), 28-34. https://doi.org/10.1016/j.ijleo.2018.06.041

Dhamodharan, P., Chen, J., & Manoharan, C. (2021). Fabrication of dye-sensitized solar cells with ZnO nanorods as photoanode and natural dye extract as sensitizer. *Journal of Materials Science: Materials in Electronics*, *32*(10), 13418-13429. https://doi.org/10.1007/s10854-021-05920-8

Dhorkule, M., Lamrood, P., Ralegankar, S., Patole, S. P., Wagh, S. S., & Pathan, H. M. (2024). Unveiling the efficiency of dye-sensitized solar cells: a journey from synthetic to natural dyes. *ES Food & Agroforestry*, *16*(2), 1-21. http://dx.doi.org/10.30919/esfaf1086

Domenici, S., Speranza, R., Bella, F., Lamberti, A., & Gatti, T. (2025). A Sustainable Hydrogel-Based Dye-Sensitized Solar Cell Coupled to an Integrated Supercapacitor for Direct Indoor Light-Energy Storage. *Solar RRL*, *9*(6), 1-10. https://doi.org/10.1002/solr.202400838

Elnemr, A.-M., Ghander, A., El-Sayed, I. A., & Elbohy, H. (2023). The effect of different concentrations of molybdenum trioxide in electrolyte for dye-sensitized solar cells (DSSCs): performance enhancement of DSSCs. *IEEE Journal of Photovoltaics*, *14*(1), 99-106. https://doi.org/10.1109/JPHOTOV.2023.3324186

Ezike, S. C., Hyelnasinyi, C. N., Salawu, M. A., Wansah, J. F., Ossai, A. N., & Agu, N. N. (2021a). Synergestic effect of chlorophyll and anthocyanin Co-sensitizers in TiO2-based dye-sensitized solar cells. *Surfaces and Interfaces*, *22*(2), 1-38. https://doi.org/10.1016/j.surfin.2020.100882

Ezike, S. C., Hyelnasinyi, C. N., Salawu, M. A., Wansah, J. F., Ossai, A. N., & Agu, N. N. (2021b). Synergestic effect of chlorophyll and anthocyanin Co-sensitizers in TiO2-based dye-sensitized solar cells. *Surfaces and Interfaces*, *22*(1), 1-12. https://doi.org/10.1016/j.surfin.2020.100882

Fan, R., Mi, Z., & Shen, M. (2019). Silicon based photoelectrodes for photoelectrochemical water splitting. *Optics express*, *27*(4), 51-80. https://doi.org/10.1364/OE.27.000A51

Fauziah, T., & Suryani, O. (2024). Betalains as Natural Dyes and Applications. *Sains Natural: Journal of Biology and Chemistry*, *14*(4), 198-209. https://doi.org/10.31938/jsn.v14i4.737

Ferreira, B., Babu, R. S., da Conceição, L., da Cunha, H., Sampaio, D., Samyn, L., & de Barros, A. (2022). Performance evaluation of DSSCs using naturally extracted dyes from petals of Lantana repens and Solidago canadensis flowers as light-harvesting units. *Ionics*, *28*(11), 5233-5242. https://doi.org/10.1007/s11581-022-04727-9

Fetouh, H., Dissouky, A., Salem, H., Fathy, M., Anis, B., & Hady Kashyout, A. (2024). Synthesis, characterization and evaluation of new alternative ruthenium complex for dye sensitized solar cells. *Scientific Reports*, *14*(1), 1-13. https://doi.org/10.1038/s41598-024-66808-1

Friedman, R. M. (2022). The 100th Anniversary of Einstein's Nobel Prize: Facts and Fiction. *Annalen der Physik*, *534*(11), 1-9. https://doi.org/10.1002/andp.202200305

Fryer, T. (2018). Life after silicon. *Engineering & Technology*, *13*(9), 62-65. https://doi.org/10.1049/et.2018.0907

Gao, W., Liu, T., Li, J., Xiao, Y., Zhang, G., Chen, Y.,…Yang, C. (2019). Simultaneously increasing open-circuit voltage and short-circuit current to minimize the energy loss in organic solar cells via designing asymmetrical non-fullerene acceptor. *Journal of Materials Chemistry A*, *7*(18), 11053-11061. https://doi.org/10.1039/C9TA02283J

Gokilamani, N., Muthukumarasamy, N., Thambidurai, M., Ranjitha, A., & Velauthapillai, D. (2013). Utilization of natural anthocyanin pigments as photosensitizers for dye-sensitized solar cells. *Journal of sol-gel science and technology*, *66*(2), 212-219. https://doi.org/10.1007/s10971-013-2994-9

Golshan, M., Osfouri, S., Azin, R., Jalali, T., & Moheimani, N. R. (2021). Co-sensitization of natural and low-cost dyes for efficient panchromatic light-harvesting using dye-sensitized solar cells. *Journal of Photochemistry and Photobiology A: Chemistry*, *417*(7), 1-11. https://doi.org/10.1016/j.jphotochem.2021.113345

Gu, Y., Liang, W., Che, Y., Cai, Z., Xiao, P., Yang, J.,…Chen, T. (2024). Solvent annealing enabling reconstruction of cadmium sulfide film for improved heterojunction quality and photovoltaic performance of antimony selenosulfide solar cells. *Advanced Functional Materials*, *34*(12), 1-15. https://doi.org/10.1002/adfm.202311577

Gupta, P. K., & Mishra, L. (2020). Ecofriendly ruthenium-containing nanomaterials: synthesis, characterization, electrochemistry, bioactivity and catalysis. *Nanoscale Advances*, *2*(5), 1774-1791. https://doi.org/10.1039/D0NA00051E

Habis, C., Zaraket, J., & Aillerie, M. (2022). Transparent conductive oxides. Part II. Specific focus on ITO, ZnO-AZO, SnO2-FTO families for photovoltaics applications. *Defect and Diffusion Forum*, *147*(2), 257-272. https://doi.org/10.4028/p-6fqmfi

Hadar, I., Song, T. B., Ke, W., & Kanatzidis, M. G. (2019). Modern processing and insights on selenium solar cells: the world's first photovoltaic device. *Advanced Energy Materials*, *9*(16), 1-9. https://doi.org/10.1002/aenm.201802766

Hakki, H. K., Allahyari, S., Rahemi, N., & Tasbihi, M. (2018). The role of thermal annealing in controlling morphology, crystal structure and adherence of dip coated TiO2 film on glass and its photocatalytic activity. *Materials Science in Semiconductor Processing*, *85*(1), 24-32. https://doi.org/10.1016/j.mssp.2018.05.031

Hasan, A. M., & Susan, M. A. B. H. (2025). PEDOT: PSS polymer functionalized carbon nanotubes integrated with graphene oxide and titanium dioxide counter electrode for dye-sensitized solar cells. *Heliyon*, *11*(3), 1-12. https://doi.org/10.1016/j.heliyon.2025.e42272

Hezarkhani, Z., & Ghadari, R. (2025). Influence of Plasmonic Au@ Cl/N Co-doped Carbon Dots on the Performance of Dye-Sensitized Solar Cells. *Applied Organometallic Chemistry*, *39*(2), 1-17. https://doi.org/10.1002/aoc.7813

Hossain, M. K., Pervez, M., Uddin, M. J., Tayyaba, S., Mia, M., Bashar, M.,…Khan, M. A. (2018). Influence of natural dye adsorption on the structural, morphological and optical properties of TiO2 based photoanode of dye-sensitized solar cell. *Mater. Sci*, *36*(1), 93-101. https://doi.org/10.1515/msp-2017-0090

Hosseinnezhad, M., Movahedi, J., & Nasiri, S. (2020). High stability photosensitizers for dye-sensitized solar cells: Synthesis, characterization and optical performance. *Optical Materials*, *109*(3), 1-17. https://doi.org/10.1016/j.optmat.2020.110198

Huang, S., Li, Q., Li, S., Li, C., Tan, H., & Xie, Y. (2024). Recent advances in the approaches for improving the photovoltaic performance of porphyrin-based DSSCs. *Chemical Communications*, *60*(34), 4521-4536. https://doi.org/10.1039/D3CC06299F

Hupfer, M., Wahyuono, R. A., Dietzek-Ivanšić, B., & Plentz, J. (2025). Co-sensitization of red and blue for dye-sensitized solar cells: A sequential approach. *Journal of Chemical Sciences*, *137*(1), 1-7. https://doi.org/10.1007/s12039-024-02330-1

Hwang, J., Matsumoto, K., Chen, C.-Y., & Hagiwara, R. (2021). Pseudo-solid-state electrolytes utilizing the ionic liquid family for rechargeable batteries. *Energy & Environmental Science*, *14*(11), 5834-5863. https://doi.org/10.1039/D1EE02567H

Ikpesu, J. E., Iyuke, S. E., Daramola, M., & Okewale, A. O. (2020). Synthesis of improved dye-sensitized solar cell for renewable energy power generation. *Solar Energy*, *206*(3), 918-934. https://doi.org/10.1016/j.solener.2020.05.002

Jaafar, H., Ain, M. F., & Ahmad, Z. A. (2018). Performance of E. conferta and G. atroviridis fruit extracts as sensitizers in dye-sensitized solar cells (DSSCs). *Ionics*, *24*(1), 891-899. https://doi.org/10.1007/s11581-017-2244-1

Jabeen, M., Mutaza, I., & Anwar, R. (2025). DSSC sensitizers: A Panoramic comparison. *Journal of the Turkish Chemical Society Section A: Chemistry*, *12*(1), 35-46. https://doi.org/10.18596/jotcsa.1467947

Jagtap, C. V., Kadam, V. S., Mahadik, M. A., Jang, J. S., & Pathan, H. M. (2021). Effect of binder concentration and dye loading time on titania based photoanode in dye sensitized solar cell application. *Engineered Science*, *17*(5), 133-141. http://dx.doi.org/10.30919/es8d581

Jaison, A. M. C., Vasudevan, D., Ponmudi, K., George, A., & Varghese, A. (2023). One pot hydrothermal synthesis and application of bright-yellow-emissive carbon quantum dots in Hg2+ detection. *Journal of Fluorescence*, *33*(6), 2281-2294. https://doi.org/10.1007/s10895-023-03233-z

Javed, H. M. A., Qureshi, A. A., Mehmood, R., Tahir, M. I., Javed, S., Sarfaraz, M.,…Ali, U. (2021). Hydrogen treated TiO2 nanoparticles onto FTO glass as photoanode for dye-sensitized solar cells with remarkably enhanced performance. *International Journal of Hydrogen Energy*, *46*(27), 14311-14321. https://doi.org/10.1016/j.ijhydene.2021.01.184

Ji, J.-M., Zhou, H., & Kim, H. K. (2018). Rational design criteria for D–π–A structured organic and porphyrin sensitizers for highly efficient dye-sensitized solar cells. *Journal of Materials Chemistry A*, *6*(30), 14518-14545. https://doi.org/10.1039/C8TA02281J

Joseph, I., Louis, H., Unimuke, T., Etim, I., Orosun, M., & Odey, J. (2020). An overview of the operational principles, light harvesting and trapping technologies, and recent advances of the dye sensitized solar cells. *Applied Solar Energy*, *56*(5), 334-363. https://doi.org/10.3103/S0003701X20050072

Kaliramna, S., Dhayal, S. S., Chaudhary, R., Khaturia, S., Ameta, K. L., & Kumar, N. (2022). A review and comparative analysis of different types of dyes for applications in dye-sensitized solar cells. *Brazilian Journal of Physics*, *52*(4), 1-17. https://doi.org/10.1007/s13538-022-01109-4

Kandregula, G. R., Mandal, S., & Pasala, V. (2025). Rapid Dye Loading Techniques in Dye-Sensitized Solar Cells. *ChemistrySelect*, *10*(5), 1-20. https://doi.org/10.1002/slct.202400082

Kapadnis, R., Bansode, S., Supekar, A., Bhujbal, P., Kale, S., Jadkar, S., & Pathan, H. (2020). Cadmium telluride/cadmium sulfide thin films solar cells: a review. *ES Energy & Environment*, *10*(20), 3-12. https://dx.doi.org/10.30919/esee8c706

Kashif, M., Ngaini, Z., Harry, A. V., Vekariya, R. L., Ahmad, A., Zuo, Z.,…Alarifi, A. (2020). An experimental and DFT study on novel dyes incorporated with natural dyes on titanium dioxide (TiO2) towards solar cell application. *Applied Physics A*, *126*(9), 1-19. https://doi.org/10.1007/s00339-020-03896-6

Kataria, V., & Mehta, D. S. (2022). Multispectral harvesting rare-earth oxysulphide based highly efficient transparent luminescent solar concentrator. *Journal of Rare Earths*, *40*(1), 41-48. https://doi.org/10.1016/j.jre.2020.09.021

Kautsar, A., Wahyuni, W. T., Syafitri, U. D., Muflihah, S., Mawadah, N., Rohaeti, E.,…Rohman, A. (2021). Data fusion of UV-Vis and FTIR spectra combined with principal component analysis for distinguishing of Andrographis paniculata extracts based on cultivation ages and solvent extraction. *Indonesian Journal of Chemistry*, *21*(3), 753-760. https://doi.org/10.22146/ijc.60321

Keremane, K. S., Abdellah, I. M., Naik, P., El-Shafei, A., & Adhikari, A. V. (2020). Simple thiophene-bridged D–π–A type chromophores for DSSCs: a comprehensive study of their sensitization and co-sensitization properties. *Physical Chemistry Chemical Physics*, *22*(40), 23169-23184. https://doi.org/10.1039/D0CP02781B

Khajavian, R., Mirzaei, M., & Alizadeh, H. (2020). Current status and future prospects of metal–organic frameworks at the interface of dye-sensitized solar cells. *Dalton Transactions*, *49*(40), 13936-13947. https://doi.org/10.1039/D0DT02798G

Kharboot, L. H., Fadil, N. A., Bakar, T. A. A., Najib, A. S. M., Nordin, N. H., & Ghazali, H. (2023). A review of transition metal sulfides as counter electrodes for dye-sensitized and quantum dot-sensitized solar cells. *Materials*, *16*(7), 1-27. https://doi.org/10.3390/ma16072881

Kharkwal, D., & Dhawan, A. (2024). Enhanced performance of dye-sensitized solar cells by mixing of metal-complex dyes. *Journal of Electronic Materials*, *53*(9), 5334-5339. https://doi.org/10.1007/s11664-024-11250-2

Kharkwal, D., Sharma, N., Gupta, S. K., & Negi, C. M. S. (2021). Enhanced performance of dye-sensitized solar cells by co-sensitization of metal-complex and organic dye. *Solar Energy*, *230*(4), 1133-1140. https://doi.org/10.1016/j.solener.2021.11.037

Kodji, N., Souop Tala Foadin, C., Mohammadou, S., Tchangnwa Nya, F., & Ejuh, G. W. (2025). Implementation of bridged copolymerisation to optimise the optical properties

of porphyrin: applications in dye-sensitized solar cells. *Molecular Physics*, *123*(1), 1-24. https://doi.org/10.1080/00268976.2024.2345727

Kokkonen, M., Talebi, P., Zhou, J., Asgari, S., Soomro, S. A., Elsehrawy, F.,…Hashmi, S. G. (2021). Advanced research trends in dye-sensitized solar cells. *Journal of Materials Chemistry A*, *9*(17), 10527-10545. https://doi.org/10.1039/D1TA00690H

Korir, B. K., Kibet, J. K., & Ngari, S. M. (2024). A review on the current status of dye-sensitized solar cells: Toward sustainable energy. *Energy Science & Engineering*, *12*(8), 3188-3226. https://doi.org/10.1002/ese3.1815

Krishna, N. V., Krishna, J. V. S., Singh, S. P., Giribabu, L., Han, L., Bedja, I.,…Islam, A. (2017). Donor-π–Acceptor based stable porphyrin sensitizers for dye-sensitized solar cells: effect of π-conjugated spacers. *The Journal of Physical Chemistry C*, *121*(12), 6464-6477. https://doi.org/10.1021/acs.jpcc.6b12869

Kumar, D. K., Kříž, J., Bennett, N., Chen, B., Upadhayaya, H., Reddy, K. R., & Sadhu, V. (2020). Functionalized metal oxide nanoparticles for efficient dye-sensitized solar cells (DSSCs): A review. *Materials Science for Energy Technologies*, *3*, 472-481. https://doi.org/10.1016/j.mset.2020.03.003

Kumar, N. S., & Naidu, K. C. B. (2021). A review on perovskite solar cells (PSCs), materials and applications. *Journal of Materiomics*, *7*(5), 940-956. https://doi.org/10.1016/j.jmat.2021.04.002

Kumarage, G. W., Hakkoum, H., & Comini, E. (2023). Recent advancements in TiO2 nanostructures: Sustainable synthesis and gas sensing. *Nanomaterials*, *13*(8), 1-10. https://doi.org/10.3390/nano13081424

Kusumawati, N., Rahmawati, K., Setiarso, P., Muslim, S., Zakiyah, N., & Fachrirakarsie, F. F. (2025). Optimizing Dye-Sensitized Solar Cell Efficiency with a Triple Blend of Caesalpinia sappan L., Dracaena angustifolia, and Clitoria ternatea L. *Molekul*, *20*(1), 73-85. https://doi.org/10.20884/1.jm.2025.20.1.12063

Kwaśnicki, P., Gronba-Chyła, A., Generowicz, A., Ciuła, J., Makara, A., & Kowalski, Z. (2024). Characterization of the TCO layer on a glass surface for PV IInd and IIIrd generation applications. *Energies*, *17*(13), 1-12.

Lee, H., Kim, J., Kim, D. Y., & Seo, Y. (2018). Co-sensitization of metal free organic dyes in flexible dye sensitized solar cells. *Organic Electronics*, *52*(4), 103-109. https://doi.org/10.1016/j.orgel.2017.10.003

Lee, M. H., Chen, Y. C., Chang, Y. M., & Hou, B. (2025). Investigation of Short-Circuit Current Density in Non-Fullerene-Based Ternary Organic Solar Cells by Incorporating

Machine Learning Algorithms with Effective Descriptors. *Solar RRL*, *9*(10), 1-22. https://doi.org/10.1002/solr.202500167

Li, H.-C., Tang, X., Yang, S.-Y., Qu, Y.-K., Jiang, Z.-Q., & Liao, L.-S. (2021). Spatial donor/acceptor architecture for intramolecular charge-transfer emitter. *Chinese Chemical Letters*, *32*(3), 1245-1248. https://doi.org/10.1016/j.cclet.2020.08.045

Li, L., Zhang, J., Deng, Z., Su, Z., Bai, Y., & He, J. (2024). Determination of phosphate in food based on molybdenum yellow derivatization coupled with resonance Rayleigh scattering method. *Analytical Sciences*, *40*(3), 461-469. https://doi.org/10.1007/s44211-023-00477-4

Li, N., Wang, Q., Zhou, J., Li, S., Liu, J., & Chen, H. (2022). Insight into the progress on natural dyes: sources, structural features, health effects, challenges, and potential. *Molecules*, *27*(10), 1-34. https://doi.org/10.3390/molecules27103291

Liang, B., Chen, X., Wang, X., Yuan, H., Sun, A., Wang, Z.,…Zhang, X. (2025). Progress in crystalline silicon heterojunction solar cells. *Journal of Materials Chemistry A*, *13*(4), 2441-2477. https://doi.org/10.1039/D4TA06224H

Lin, L., Bora, B., Prasad, B., Sastry, O., Mondal, S., & Ravindra, N. (2023). Influence of outdoor conditions on PV module performance—An overview. *Material Science & Engineering International Journal*, *7*(2), 88-101. https://doi.org/10.15406/mseij.2023.07.00210

Lin, Y.-S., & Chen, W.-H. (2025). Dye-Sensitized Solar Cells with Modified TiO2 Scattering Layer Produced by Hydrothermal Method. *Materials*, *18*(2), 1-13. https://doi.org/10.3390/ma18020278

Liu, B.-Q., Zhao, X.-P., & Luo, W. (2008). The synergistic effect of two photosynthetic pigments in dye-sensitized mesoporous TiO2 solar cells. *Dyes and pigments*, *76*(2), 327-331. https://doi.org/10.1016/j.dyepig.2006.09.004

Liu, Y., Dai, X., Li, J., Cheng, S., Zhang, J., & Ma, Y. (2024). Recent progress in TiO 2–biochar-based photocatalysts for water contaminants treatment: strategies to improve photocatalytic performance. *RSC advances*, *14*(1), 478-491. https://doi.org/10.1039/D3RA06910A

Lu, W., Shi, Y., Wang, R., Su, D., Tang, M., Liu, Y., & Li, Z. (2021). Antioxidant activity and healthy benefits of natural pigments in fruits: A review. *International journal of molecular sciences*, *22*(9), 1-18. https://doi.org/10.3390/ijms22094945

Lukong, V., Ukoba, K., Yoro, K., & Jen, T. (2022). Annealing temperature variation and its influence on the self-cleaning properties of TiO2 thin films. *Heliyon*, *8*(5), 1-9. https://doi.org/10.1016/j.heliyon.2022.e09460

M Atia, D., Ahmed, N. M., Abou Hammad, A. B., Toraya, M. M., & El Nahrawy, A. M. (2025). Reduced Graphene Oxide/Cobalt Sulfide/Titinum-Zirconiate for Dye-Sensitized Solar Cell. *Egyptian Journal of Chemistry*, *68*(5), 419-430. https://doi.org/10.21608/ejchem.2024.314249.10258

Machín, A., & Márquez, F. (2024). Advancements in photovoltaic cell materials: silicon, organic, and perovskite solar cells. *Materials*, *17*(5), 1-42. https://doi.org/10.3390/ma17051165

Magiswaran, K., Norizan, M. N., Mahmed, N., Mohamad, I. S., Idris, S. N., Sabri, M. F. M.,…Nabiałek, M. (2022). Controlling the layer thickness of zinc oxide photoanode and the dye-soaking time for an optimal-efficiency dye-sensitized solar cell. *Coatings*, *13*(1), 1-20. https://doi.org/10.3390/coatings13010020

Magiswaran, K., Norizan, M. N., Mohamad, I. S., Mahmed, N., Idris, S. N., & Sobri, S. A. (2021). Charge Recombination in Zinc Oxide-Based Dye-Sensitized Solar Cell: A Mini Review. *International Journal of Nanoelectronics & Materials*, *14*(3), 59-66.

Malhotra, S. S., Ahmed, M., Gupta, M. K., & Ansari, A. (2024). Metal-free and natural dye-sensitized solar cells: recent advancements and future perspectives. *Sustainable Energy & Fuels*, *8*(18), 4127-4163. https://doi.org/10.1039/D4SE00406J

Malumi, S. O., Malumi, T., Osiele, M. O., Ekpekpo, A., & Ikhioya, I. L. (2023). Enhance and performance evolution of silver-doped titanium dioxide dye-sensitized solar cells using different dyes. *Journal of Engineering in Industrial Research*, *4*(4), 189-200. https://doi.org/10.48309/JEIRES.2023.4.1

Manikandan, M., Anooja, J., Narayanan Unni, K., & Sujatha Devi, P. (2025). Enhancing light harvesting in bilayered dye-sensitized solar cells by tailoring light scattering with electrospun TiO 2 nanofibers. *RSC advances*, *15*(8), 6171-6182. https://doi.org/10.1039/D4RA08679A

Manz, N. B., & Fuierer, P. A. (2023). Mathematical Approach to Optimizing the Panchromatic Absorption of Natural Dye Combinations for Dye-Sensitized Solar Cells. *Colorants*, *2*(1), 90-110. https://doi.org/10.3390/colorants2010007

Mariotti, N., Bonomo, M., Fagiolari, L., Barbero, N., Gerbaldi, C., Bella, F., & Barolo, C. (2020). Recent advances in eco-friendly and cost-effective materials towards

sustainable dye-sensitized solar cells. *Green chemistry*, *22*(21), 7168-7218. https://doi.org/10.1039/D0GC01148G

Masud, & Kim, H. K. (2023). Redox shuttle-based electrolytes for dye-sensitized solar cells: comprehensive guidance, recent progress, and future perspective. *ACS omega*, *8*(7), 6139-6163. https://doi.org/10.1021/acsomega.2c06843

Matsumura, M., Matsudaira, S., Tsubomura, H., Takata, M., & Yanagida, H. (1980). Dye sensitization and surface structures of semiconductor electrodes. *Industrial & Engineering Chemistry Product Research and Development*, *19*(3), 415-421. https://doi.org/10.1021/i360075a025

Mauri, L., Colombo, A., Dragonetti, C., Roberto, D., & Fagnani, F. (2021). Recent investigations on thiocyanate-free ruthenium (II) 2, 2′-bipyridyl complexes for dye-sensitized solar cells. *Molecules*, *26*(24), 1-12. https://doi.org/10.3390/molecules26247638

Mejica, G. F. C., Ramaraj, R., & Unpaprom, Y. (2022). Natural dye (chlorophyll, anthocyanin, carotenoid, flavonoid) photosensitizer for dye-sensitized solar cell: A review. *Maejo International Journal of Energy and Environmental Communication*, *4*(1), 12-22. https://doi.org/10.54279/mijeec.v4i1.247970

Melo Miranda, B., Vilela Junior, O., Santos Fernandes, S., Mendes Lemos, G. R., Schwan, C. L., Aliaño-González, M. J.,…Murowaniecki Otero, D. (2025). Potential of New Plant Sources as Raw Materials for Obtaining Natural Pigments/Dyes. *Agronomy*, *15*(2), 1-30. https://doi.org/10.3390/agronomy15020405

Meng, L., You, J., & Yang, Y. (2018). Addressing the stability issue of perovskite solar cells for commercial applications. *Nature communications*, *9*(1), 1-4. https://doi.org/10.1038/s41467-018-07255-1

Meyer, E., Taziwa, R., Mutukwa, D., & Zingwe, N. (2018). A review on the advancement of ternary alloy counter electrodes for use in dye-sensitised solar cells. *Metals*, *8*(12), 1-22. https://doi.org/10.3390/met8121080

Mohsen, M. K., Rahman, A. S. A. A., Abdullah, N. R., & Hashim, A. A. (2021). Synthesis and Investigation of Metals Oxide Pastes Used as Semiconductors Electrode for Dye-sensitized Solar Cells. *NeuroQuantology*, *19*(10), 41-47.

Müller, A. V., Wierzba, W. M., Pastorelli, M. N., & Polo, A. S. (2021). Interfacial electron transfer in dye-sensitized TiO2 devices for solar energy conversion. *Journal of the Brazilian Chemical Society*, *32*(9), 1711-1738. https://doi.org/10.21577/0103-5053.20210083

Mulya Harahap, R. I., Kurniati, I., Suraya, N., Rostini, T., Ropii, B., & Bethasari, M. (2025). Comparative Analysis of Serum Magnesium Ion Levels Using Three Measurement Methods: Spectrophotometry, Atomic Absorption Spectrophotometry, and Inductively Coupled Plasma With Optical Emission Spectrophotometry. *International Journal of Analytical Chemistry*, *5*(1), 1-12. https://doi.org/10.1155/ianc/8853568

Muthee, D. K., & Dejene, B. F. (2021). Effect of annealing temperature on structural, optical, and photocatalytic properties of titanium dioxide nanoparticles. *Heliyon*, *7*(6), 1-12. https://doi.org/10.1016/j.heliyon.2021.e07269

Nagaraj, K., Radha, S., Deepa, C. G., Raja, K., Umapathy, V., Badgujar, N. P.,…Uthra, C. (2025). Photocatalytic advancements and applications of titanium dioxide (TiO_2): Progress in biomedical, environmental, and energy sustainability. *Next Research*, *2*(1), 1-10. https://doi.org/10.1016/j.nexres.2025.100180

Najm, A. S., Alwash, S. A., Sulaiman, N. H., Chowdhury, M., & Techato, K. (2023). N719 dye as a sensitizer for dye-sensitized solar cells (DSSCs): A review of its functions and certain rudimentary principles. *Environmental Progress & Sustainable Energy*, *42*(1), 1-19. https://doi.org/10.1002/ep.13955

Nalzala Thomas, M. R., Kanniyambatti Lourdusamy, V. J., Dhandayuthapani, A. A., & Jayakumar, V. (2021). Non-metallic organic dyes as photosensitizers for dye-sensitized solar cells: a review. *Environmental Science and Pollution Research*, *28*(23), 28911-28925. https://doi.org/10.1007/s11356-021-13751-7

O'regan, B., & Grätzel, M. (1991). A low-cost, high-efficiency solar cell based on dye-sensitized colloidal TiO2 films. *nature*, *353*(6346), 737-740. https://doi.org/10.1038/353737a0

Omar, A., Ali, M. S., & Abd Rahim, N. (2020). Electron transport properties analysis of titanium dioxide dye-sensitized solar cells (TiO2-DSSCs) based natural dyes using electrochemical impedance spectroscopy concept: A review. *Solar Energy*, *207*(1), 1088-1121. https://doi.org/10.1016/j.solener.2020.07.028

Onah, E. O., Onuorah, M., Offiah, S., Obodo, R. M., Ekechukwu, O., Ugwuoke, P., & Ezema, F. I. (2021). Effects of annealing temperature on TiO 2 photoelectrodes of dye-sensitized solar cells using Ixora coccenia dye extract. *Journal of Nanoparticle Research*, *23*(2), 1-14. https://doi.org/10.1007/s11051-021-05335-w

Onyemowo, M., Unpaprom, Y., & Ramaraj, R. (2024). Exploring the potential of natural dyes in DSSCs: Innovations for efficient light harvesting and charge separation through Co-

sensitization. *Optical Materials*, *148*(1), 1-6. https://doi.org/10.1016/j.optmat.2024.114860

Orona-Navar, A., Aguilar-Hernández, I., Nigam, K., Cerdán-Pasarán, A., & Ornelas-Soto, N. (2021). Alternative sources of natural pigments for dye-sensitized solar cells: Algae, cyanobacteria, bacteria, archaea and fungi. *Journal of Biotechnology*, *332*(8), 29-53. https://doi.org/10.1016/j.jbiotec.2021.03.013

Ossai, A. N., Ezike, S. C., Timtere, P., & Ahmed, A. D. (2021). Enhanced photovoltaic performance of dye-sensitized solar cells-based Carica papaya leaf and black cherry fruit co-sensitizers. *Chemical Physics Impact*, *2*(1), 1-8. https://doi.org/10.1016/j.chphi.2021.100024

Pallikkara, A., & Ramakrishnan, K. (2021). Efficient charge collection of photoanodes and light absorption of photosensitizers: A review. *International Journal of Energy Research*, *45*(2), 1425-1448. https://doi.org/10.1002/er.5941

Pant, B., Park, M., & Park, S.-J. (2019). Recent advances in TiO2 films prepared by sol-gel methods for photocatalytic degradation of organic pollutants and antibacterial activities. *Coatings*, *9*(10), 1-20. https://doi.org/10.3390/coatings9100613

Park, J. M., Hong, K.-I., Lee, H., & Jang, W.-D. (2021). Bioinspired applications of porphyrin derivatives. *Accounts of chemical research*, *54*(9), 2249-2260. https://doi.org/10.1021/acs.accounts.1c00114

Pashaei, B., Shahroosvand, H., Graetzel, M., & Nazeeruddin, M. K. (2016). Influence of ancillary ligands in dye-sensitized solar cells. *Chemical reviews*, *116*(16), 9485-9564. https://doi.org/10.1021/acs.chemrev.5b00621

Patni, N., G. Pillai, S., & Sharma, P. (2020). Effect of using betalain, anthocyanin and chlorophyll dyes together as a sensitizer on enhancing the efficiency of dye-sensitized solar cell. *International Journal of Energy Research*, *44*(13), 10846-10859. https://doi.org/10.1002/er.5752

Periyasamy, K., Sakthivel, P., Venkatesh, G., Vennila, P., Mary, Y. S., & Haseena, S. (2024). Structural and photophysical studies of triphenylamine-based organic dyes for applications in DSSCs: experimental and DFT analysis. *Polycyclic Aromatic Compounds*, *44*(8), 5314-5337. https://doi.org/10.1080/10406638.2023.2264450

Pinheiro, X., Vilanova, A., Mesquita, D., Monteiro, M., Eriksson, J., Barbosa, J.,…Capitão, J. (2023). Design of experiments optimization of fluorine-doped tin oxide films prepared by spray pyrolysis for photovoltaic applications. *Ceramics International*, *49*(8), 13019-13030. https://doi.org/10.1016/j.ceramint.2022.12.175

Pirdaus, N. A., Ahmad, N., Dahlan, N. Y., Redzuan, A. N., Zalizan, A. H., Muhammad-Sukki, F.,…Wan-Mohtar, W. A. A. Q. I. (2024). Performance of yellow and pink oyster mushroom dyes in dye sensitized solar cell. *Scientific Reports*, *14*(1), 1-19. https://doi.org/10.1038/s41598-024-73865-z

Ponnambalam, S., Junluthin, P., Ramaraj, R., & Unpaprom, Y. (2023). Investigating the effect of solvent on the efficiency of natural pigment-based dye-sensitized solar cells. *Maejo International Journal of Energy and Environmental Communication*, *5*(1), 20-25. https://doi.org/10.54279/mijeec.v5i1.250547

Pratiwi, R. A., & Nandiyanto, A. B. D. (2022). How to read and interpret UV-VIS spectrophotometric results in determining the structure of chemical compounds. *Indonesian Journal of Educational Research and Technology*, *2*(1), 1-20.

Qiao, J., Hu, W., Chen, S., Cui, H., Qi, J., Yu, Y.,…Wang, J. (2025). Effect of LED Lights on Morphological Construction and Leaf Photosynthesis of Lettuce (Lactuca sativa L.). *Horticulturae*, *11*(1), 1-21. https://doi.org/10.3390/horticulturae11010043

Qurratulain, Kazmi, S. A., Hameed, S., Pachauri, R. K., Khan, B., & Ali, A. (2025). Study on dye-sensitized solar cell efficiency improvement using methyl orange dye. *Materials for Renewable and Sustainable Energy*, *14*(1), 1-8. https://doi.org/10.1007/s40243-025-00296-9

Ragab, M. M., Hassabo, A. G., & Othman, H. (2022). An overview of natural dyes extraction techniques for valuable utilization on textile fabrics. *Journal of Textiles, Coloration and Polymer Science*, *19*(2), 137-153. https://doi.org/10.21608/jtcps.2022.130253.1115

Rahman, S., Haleem, A., Siddiq, M., Hussain, M. K., Qamar, S., Hameed, S., & Waris, M. (2023). Research on dye sensitized solar cells: recent advancement toward the various constituents of dye sensitized solar cells for efficiency enhancement and future prospects. *RSC advances*, *13*(28), 19508-19529. https://doi.org/10.1039/D3RA00903C

Rajaramanan, T., Heidari Gourji, F., Elilan, Y., Yohi, S., Senthilnanthanan, M., Ravirajan, P., & Velauthapillai, D. (2023). Natural sensitizer extracted from Mussaenda erythrophylla for dye-sensitized solar cell. *Scientific Reports*, *13*(1), 1-13. https://doi.org/10.1038/s41598-023-40437-6

Raouafi, A., Jbahi, S., Bessalah, S., Daoudi, M., Dridi, W., Hamzaoui, A. H.,…Hidouri, M. (2022). Natural red dyes from Beta vulgaris L. extract for gamma-rays color indicator: Physico-chemical and biological characterizations. *Journal of the Indian Chemical Society*, *99*(10), 1-7. https://doi.org/10.1016/j.jics.2022.100722

Reza, K. M., Kurny, A., & Gulshan, F. (2017). Parameters affecting the photocatalytic degradation of dyes using TiO2: a review. *Applied Water Science*, *7*(4), 1569-1578. https://doi.org/10.1007/s13201-015-0367-y

Roslan, N., Ya'acob, M., Radzi, M., Hashimoto, Y., Jamaludin, D., & Chen, G. (2018). Dye Sensitized Solar Cell (DSSC) greenhouse shading: New insights for solar radiation manipulation. *Renewable and Sustainable Energy Reviews*, *92*(5), 171-186. https://doi.org/10.1016/j.rser.2018.04.095

Rotich, V., Wangila, P., & Cherutoi, J. (2022). FT-IR Analysis of Beta vulgaris Peels and Pomace Dye Extracts and Surface Analysis of Optimally Dyed-Mordanted Cellulosic Fabrics. *Journal of Chemistry*, *22*(1), 1-12. https://doi.org/10.1155/2022/2233414

Ruba, N., Prakash, P., Sowmya, S., Janarthana, B., Prabu, A. N., Chandrasekaran, J.,…Yahia, I. (2021). Recent advancement in photo-anode, dye and counter cathode in dye-sensitized solar cell: a review. *Journal of Inorganic and Organometallic Polymers and Materials*, *31*(4), 1894-1901. https://doi.org/10.1007/s10904-020-01854-6

Ruhane, T., Islam, M. T., Rahaman, M. S., Bhuiyan, M., Islam, J. M., Newaz, M.,…Khan, M. A. (2017). Photo current enhancement of natural dye sensitized solar cell by optimizing dye extraction and its loading period. *Optik*, *149*(1), 174-183. https://doi.org/10.1016/j.ijleo.2017.09.024

Sarwar, N., Shahzad, M., Ghaffar, R., Javed, K., Munam, M., Pervez, A., & Ghaffar, A. (2023). Fabrication of DSSC based on Capsicum annuum and Tamarindus indica plant seeds extract as natural photosensitizers. *Solar Energy*, *257*, 314-323. https://doi.org/10.1016/j.solener.2023.04.039

Semalti, P., & Sharma, S. N. (2020). Dye sensitized solar cells (DSSCs) electrolytes and natural photo-sensitizers: a review. *Journal of nanoscience and nanotechnology*, *20*(6), 3647-3658. https://doi.org/10.1166/jnn.2020.17530

Semenycheva, L., Chasova, V., Matkivskaya, J., Fukina, D., Koryagin, A., Belaya, T.,…Suleimanov, E. (2021). Features of polymerization of methyl methacrylate using a photocatalyst—the complex oxide RbTe1. 5W0. 5O6. *Journal of Inorganic and Organometallic Polymers and Materials*, *31*(8), 3572-3583. https://doi.org/10.1007/s10904-021-02054-6

Sen, Y., Takmaz, A., KabakcÄ, A., KabakcÄ, G., & Deniz, G. (2018). Renewable energy and photovoltaic technology. *Journal of Engineering Research and Applied Science*, *7*(1), 739-752.

Shah, S., Abidin, Z. H. Z., Noor, I., Osman, Z., & Arof, A. (2023). Performance improvement of dye-sensitized solar cells with Ag nanoparticles. *Molecular Crystals and Liquid Crystals*, *762*(1), 88-98. https://doi.org/10.1080/15421406.2023.2180213

Sharma, P., & Mishra, R. K. (2025). Comprehensive study on photovoltaic cell's generation and factors affecting its performance: A Review. *Materials for Renewable and Sustainable Energy*, *14*(1), 1-28. https://doi.org/10.1007/s40243-024-00292-5

Singh, A., Srivastava, D., Gosavi, S. W., Chauhan, R., Ashokkumar, M., Albalwi, A. N.,…Kumar, A. (2022). A double co-sensitization strategy using heteroleptic transition metal ferrocenyl dithiocarbamate phenanthrolene-dione for enhancing the performance of N719-based DSSCs. *RSC advances*, *12*(43), 28088-28097. https://doi.org/10.1039/D2RA05601A

Sinha, D., De, D., Goswami, D., Mondal, A., & Ayaz, A. (2019). ZnO and TiO2 nanostructured dye sensitized solar photovoltaic cell. *Materials Today: Proceedings*, *11*(2), 782-788. https://doi.org/10.1016/j.matpr.2019.03.043

Sreeja, S., & Pesala, B. (2018). Co-sensitization aided efficiency enhancement in betanin–chlorophyll solar cell. *Materials for Renewable and Sustainable Energy*, *7*(4), 1-14. https://doi.org/10.1007/s40243-018-0132-x

Srivastava, K. V., Srivastava, P., Srivastava, A., Maurya, R. K., Singh, Y. P., & Srivastava, A. (2025). 1D TiO 2 photoanodes: a game-changer for high-efficiency dye-sensitized solar cells. *RSC advances*, *15*(7), 4789-4819. https://doi.org/10.1039/D4RA06254J

Sudharshan, N., & Swetha, V. (2023). UV-visible spectroscopy: a comprehensive review on instrumentation. *World Journal of Pharmaceutical Research*, *12*(19), 1342-1363. https://doi.org/10.20959/wjpr202319-30171

Syafinar, R., Gomesh, N., Irwanto, M., Fareq, M., & Irwan, Y. (2015). Chlorophyll pigments as nature based dye for dye-sensitized solar cell (DSSC). *Energy Procedia*, *79*(2), 896-902. https://doi.org/10.1016/j.egypro.2015.11.584

Syrek, K., Sennik-Kubiec, A., Rodríguez-López, J., Rutkowska, M., Żmudzki, P., Hnida-Gut, K. E.,…Sulka, G. D. (2020). Reactive and morphological trends on porous anodic TiO2 substrates obtained at different annealing temperatures. *International Journal of Hydrogen Energy*, *45*(7), 4376-4389. https://doi.org/10.1016/j.ijhydene.2019.11.213

Tamilselvan, S. N., & Shanmugan, S. (2024). Towards sustainable solar cells: unveiling the latest developments in bio-nano materials for enhanced DSSC efficiency. *Clean Energy*, *8*(3), 238-257. https://doi.org/10.1093/ce/zkae031

Teja, A. S., Srivastava, A., Satrughna, J. A. K., Tiwari, M. K., Kanwade, A., Lee, H.,…Shirage, P. M. (2023). Synergistic co-sensitization of environment-friendly chlorophyll and anthocyanin-based natural dye-sensitized solar cells: An effective approach towards enhanced efficiency and stability. *Solar Energy*, *261*(3), 112-124. https://doi.org/10.1016/j.solener.2023.06.004

Treat, N. A., Knorr, F. J., & McHale, J. L. (2016). Templated assembly of betanin chromophore on TiO2: aggregation-enhanced light-harvesting and efficient electron injection in a natural dye-sensitized solar cell. *The Journal of Physical Chemistry C*, *120*(17), 9122-9131. https://doi.org/10.1021/acs.jpcc.6b02532

Vallejo, W., Lerma, M., & Díaz-Uribe, C. (2025). Dye sensitized solar cells: Meta-analysis of effect sensitizer-type on photovoltaic efficiency. *Heliyon*, *11*(1), 1-19. https://doi.org/10.1016/j.heliyon.2024.e41092

Vinoth Kumar, J., Kavitha, G., Arulmozhi, R., Arul, V., Singaravadivel, S., & Abirami, N. (2021). Green sources derived carbon dots for multifaceted applications. *Journal of Fluorescence*, *31*(4), 915-932. https://doi.org/10.1007/s10895-021-02721-4

Wang, J., & Azam, W. (2024). Natural resource scarcity, fossil fuel energy consumption, and total greenhouse gas emissions in top emitting countries. *Geoscience frontiers*, *15*(2), 1-15. https://doi.org/10.1016/j.gsf.2023.101757

Wang, X.-L., Huang, J.-F., Liu, J.-M., & Tsiakaras, P. (2025). Recent advances in metal-free photosensitizers for dye-sensitized photoelectrochemical cells. *Coordination Chemistry Reviews*, *522(2)*, 216143-216160. https://doi.org/10.1016/j.ccr.2024.216143

Wathudura, P., Pham, H., Siriwardana, K., Athukorale, S., Jayasundara, U., Gunatilake, S. R.,…Zhang, D. (2025). Expanding the Horizons of UV–vis Spectroscopy Education: Beyond the Beer–Lambert Law. *Journal of Chemical Education*, *102*(6), 2389-2397. https://doi.org/10.1021/acs.jchemed.5c00255

Wu, J., Lan, Z., Lin, J., Huang, M., Huang, Y., Fan, L.,…Wei, Y. (2017). Counter electrodes in dye-sensitized solar cells. *Chemical Society Reviews*, *46*(19), 5975-6023. https://doi.org/10.1039/C6CS00752J

Xu, F., Gong, K., Liu, D., Wang, L., Li, W., & Zhou, X. (2022). Enhancing photocurrent of dye-sensitized solar cells through solvent modulating aggregation of dyes. *Solar Energy*, *240*, 157-167. https://doi.org/10.1016/j.solener.2022.05.032

Yadav, S., Chauhan, R., Mishra, R., & Kumar, S. (2023). Investigating Ag2S quantum dot buffer layer in CZTSSe photovoltaics for enhanced performance. *Physica Scripta*, *98*(12), 1-20. https://doi.org/10.1088/1402-4896/ad06fa

Yadav, S., Shakya, K., Gupta, A., Singh, D., Chandran, A. R., Varayil Aanappalli, A.,…Saini, K. (2023). A review on degradation of organic dyes by using metal oxide semiconductors. *Environmental Science and Pollution Research*, *30*(28), 71912-71932. https://doi.org/10.1007/s11356-022-20818-6

Yang, X., Deng, Y., Yang, H., Liao, Y., Cheng, X., Zou, Y.,…Deng, Y. (2023). Functionalization of mesoporous semiconductor metal oxides for gas sensing: Recent advances and emerging challenges. *Advanced Science*, *10*(1), 1-24. https://doi.org/10.1002/advs.202204810

Yeoh, M. E., & Chan, K. Y. (2017). Recent advances in photo-anode for dye-sensitized solar cells: a review. *International Journal of Energy Research*, *41*(15), 2446-2467. https://doi.org/10.1002/er.3764

Zaman, S. N. Y. K., & Ahmad, M. K. (2022). Transparent dye-sensitized solar cell using titanium dioxide thin film. *Evolution in Electrical and Electronic Engineering*, *3*(2), 108-117. https://doi.org/10.30880/eeee.2022.03.02.013

Zeng, J., Li, Z., Jiang, H., & Wang, X. (2021). Progress on photocatalytic semiconductor hybrids for bacterial inactivation. *Materials horizons*, *8*(11), 2964-3008. https://doi.org/10.1039/D1MH00773D

Zeng, K., Tong, Z., Ma, L., Zhu, W.-H., Wu, W., & Xie, Y. (2020). Molecular engineering strategies for fabricating efficient porphyrin-based dye-sensitized solar cells. *Energy & Environmental Science*, *13*(6), 1617-1657. https://doi.org/10.1039/C9EE04200H

Zhang, S., Zhang, X., Sun, Y., Zhou, W., Cao, W., & Cheng, D. (2023). Investigation of the annealing treatment on the performance of TiO2 photoanode. *International Journal of Hydrogen Energy*, *48*(77), 29996-30005. https://doi.org/10.1016/j.ijhydene.2023.04.196

APPENDICES

Appendix I: Research permit

REPUBLIC OF KENYA

NATIONAL COMMISSION FOR SCIENCE,TECHNOLOGY & INNOVATION

Ref No: **618918**

Date of Issue: **10/September/2025**

RESEARCH LICENSE

This is to Certify that Mr.. Zachariah kibagendi Moronge of Egerton University, has been licensed to conduct research as per the provision of the Science, Technology and Innovation Act, 2013 (Rev.2014) in Nakuru on the topic: PREPARATION AND OPTIMIZATION OF PIGMENTS FROM Spinacia oleracea, Beta vulgaris, AND Rubus fruticosus FOR APPLICATION IN DYE-SENSITIZED SOLAR CELLS for the period ending : 10/September/2026.

License No: **NACOSTI/P/25/4179042**

618918

Applicant Identification Number

Ag. Director General
NATIONAL COMMISSION FOR SCIENCE,TECHNOLOGY & INNOVATION

Verification QR Code

NOTE: This is a computer generated License. To verify the authenticity of this document, Scan the QR Code using QR scanner application.

See overleaf for conditions

Appendix II: Research publication

East African Journal of Engineering, Volume 8, Issue 2, 2025
Article DOI: https://doi.org/10.37284/eaje.8.2.3819

East African Journal of Engineering
eaje.eanso.org
Volume 8, Issue 2, 2025
Print ISSN: 2707-5389 | Online ISSN: 2707-5397
Title DOI: https://doi.org/10.37284/2707-5397

EAST AFRICAN NATURE & SCIENCE ORGANIZATION

Original Article

Effects of Co-sensitising Chlorophyll and Betanin dyes on Optical Absorption properties and Photovoltaic performance of titanium dioxide-based Dye-S

Zachariah Moronge[1], Duke Oeba[1] & Charles Muga[1]*

[1] Egerton University, P. O. Box 536-20115, Egerton, Kenya.
[*] Author for Correspondence Email: zmoronge2477@gmail.com

Article DOI : https://doi.org/10.37284/eaje.8.2.3819

Publication Date:

13 October 2025

Keywords:

DSSCS, FTIR, Natural Dyes, Co-sensitisation, Absorption, UV-Vis Spectrophotometry, PCE

ABSTRACT

To address the increasing energy demands, renewable energy technologies, such as Dye-Sensitised Solar Cells (DSSCs), are considered due to their low fabrication costs and environmental friendliness. However, to date, reduced optical absorption and low carrier collection are the primary reasons for the low Power Conversion Efficiency (PCE) of DSSCs. Previous studies have shown that natural dyes are potential sensitisers and co-sensitisers that enhance the performance of these solar cells. The present work focused on the application of natural dyes, betanin (Beta vulgaris) and chlorophyll (Spinacea oleracea), in DSSCs synthesised using titanium dioxide (TiO2) mesoporous films. The pigments were blended in a 1:1 volume ratio. The measurements of optical characteristics were performed using a UV-Vis spectrometer (400-800 nm), while an FT-IR spectrometer was used to determine functional groups. Chlorophyll had a broad absorption peak at 427 and 673 nm, whereas betanin showed a peak at 527 nm. The spectral interactions were confirmed by the shift of chlorophyll peaks to 440 and 671 nm, whereas betanin exhibited a bathochromic shift of 22 nm in the composite dye, respectively. FT-IR analysis revealed the presence of various functional groups, including O-H, C=O, C-H, and C-O, which are essential for light absorption and binding to TiO2. The co-sensitised DSSCs showed enhanced photovoltaic performance compared to the single-dye cells with a current density (JSC) of 1.22 mA/cm2, open-circuit voltage (VOC) of 0.63 V, and PCE of 0.56 %. These results demonstrate that natural dye co-sensitisation can be a practical approach for enhancing light trapping and efficiency in DSSCs, offering a sustainable alternative for solar energy applications.

APA CITATION

Moronge, Z., Oeba, D. & Muga, C. (2025). Effects of Co-sensitising Chlorophyll and Betanin dyes on Optical Absorption properties and Photovoltaic performance of titanium dioxide-based Dye-S. *East African Journal of Engineering*, *8*(2), 106-118. https://doi.org/10.37284/eaje.8.2.3819

Appendix III: Photovoltaic parameters of single-sensitized and co-sensitized DSSCs

	Natural dye	Source	Extracting solvent	J_{SC} (mA/cm^2)	V_{OC} (mV)	FF (%)	PCE (%)	Reference
1	Anthocyanin	*Ixora coccinea petals*	70% ethanol	3.005	344	0.507	0.56	(Zolkepli *et al*., 2015)
	Anthocyanin	*Tradescantia spathacea leaves*		1.189	285	0.554	0.21	
	Co-sensitized			4.185	346	0.499	0.80	
2	Curcuminoids	Turmeric powder	Ice-cold methanol	0.822	553	0.522	0.237	(Manz & Fuierer, 2023)
	Phycobilins	*Blue Spirulina plantensis* powder		0.214	523	0.660	0.073	
	Co-sensitized			0.417	538	0.647	0.145	
3	Chlorophyll-*a*	papaya	Ethanol	1.77	400	0.42	0.29	(Ossai *et al*., 2021)
	Anthocyanin	black cherry		1.56	380	0.43	0.25	
	Co-sensitized			2.15	490	0.54	0.56	
4	chlorophyll	pomegranate leaf	Alcohol	2.05	560	0.52	0.597	(Chang & Lo, 2010)
	anthocyanin	mulberry		1.89	555	0.53	0.548	
	Co-sensitized			2.8	530	0.49	0.722	
5	Anthocyanin	*H sabdariffa, Manipur*	Isopropanol	3.2	803	0.69	1.47	(Patni *et al.*, 2020)
	betalain	*B vulgaris*		4.06	578	0.66	1.29	
	chlorophyll	spinach		3.14	552	0.66	0.95	
	Co-sensitized			7.36	883	0.69	3.73	

6	chlorophyll	Chinar leaves	Acetone	0.01	468	4	0.55	(Liu *et al.*,
	xanthophyll	yellow chrysanthemum	Anhydrous ethanol + petroleum ether	0.02	479	11	2.225	2008)
	Co-sensitized			0.02	502	11	3.19	
7	anthocyanins	Fragaria	Acetone and ethanol methanol	0.08	380	46.44	0.09	(Kokkonen et al., 2021)
	chlorophyll	Mentha leaves		0.10	410	57.16	0.15	
	auxin hormone	Helianthus annuus leaves		0.19	480	50.77	0.29	
	Co-sensitized			0.25	590	73.55	0.69	
8	Anthocyanin	Purple cabbage	Ethanol solution (1:1)	0.39	521	0.5	0.1015	(Sinha *et al.*, 2020)
	chlorophyll	Spinach		0.66	400	0.5	0.1312	
	betaxanthin	Turmeric		1.2	500	0.51	0.3045	
	Co-sensitized			1.65	530	0.68	0.602	
9	Chlorophyll	Wormwood	Absolute ethanol	1.96	585	47	0.538	(Chang *et al.*,
	Anthocyanin	Purple cabbage		2.08	666	53	0.75	2013)
	Co-sensitized			3.16	666	62	1.29	